Progress in numerical simulation of yield stress fluid flows

Pierre Saramito, Anthony Wachs

Submitted manuscript No.
(will be inserted by the editor)

Progress in numerical simulation of yield stress fluid flows

Pierre Saramito[1], **Anthony Wachs**[2,3]

[1] Lab. J. Kuntzmann, CNRS and Grenoble university CS 40700, 38058 Grenoble cedex 9, France.
[2] Department of Mathematics, University of British Columbia, 1984 Mathematics Road, Vancouver, BC, Canada, V6T 1Z2.
[3] Department of Chemical and Biological Engineering, University of British Columbia, 2360 East Mall, Vancouver, BC Canada V6T 1Z3.

October 3, 2016

Abstract Numerical simulations of viscoplastic fluid flows have provided a better understanding of fundamental properties of yield stress fluids in many applications relevant of natural and engineering sciences. In the first part of this paper, we review the classical numerical methods for the solution of the non-smooth viscoplastic mathematical models, highlight their advantages and drawbacks, and discuss more recent numerical methods that show promises for fast algorithms and accurate solutions. In the second part, we present and analyze a variety of applications and extensions involving viscoplastic flow simulations: yield slip at the wall, heat transfer, thixotropy, granular materials, combining elasticity, with multiple phases and shallow flow approximations. We illustrate from a physical viewpoint how fascinating the corresponding rich phenomena pointed out by these simulations are.

Introduction

The first model for fluids with plasticity has been introduced at the end of the 19th century by Schwedoff [157] for gelatin suspensions. Schwedoff was the forerunner to a multitude of papers on variable viscosity effects in a plethora of materials which were to occupy much of the literature of the first half of the 20th century. In their historical review, Tanner and Walters [165, p. 26] pointed out that, during this period, "*there was a tendency to label all anomalous behavior as manifestations of 'plasticity', with no clear idea as to what that meant*". The work of Bingham [27,28] introduced some clarifications and provided a great deal of information on measurements for various systems, including gel-like materials with a yield stress. While this mathematical model was expressed for simple shear flow only, its extension to a general three-dimensional flow was introduced in 1947 by Oldroyd [132], based on the von Mises criterion.

Numerically simulating the flow of a yield stress material is not a straightforward task. Assuming that rheological models with a threshold in terms of the norm of the deviatoric part of the stress tensor, i.e., a von Mises criterion, represent a satisfactory approximation of the observable behavior of a material, the mathematical non-smoothness of these models and the indeterminacy of the stress tensor below the yield stress threshold render the design of appropriate solution methods subtler than for a simple purely viscous material. Over the past 40 years, essentially two families of solution methods were suggested in the literature, the so-called regularization approach and augmented Lagrangian algorithm. The former solution method circumvents the aforementioned two problematic mathematical properties by simply modifying the constitutive equation such that it is smooth and well determined regardless of the shear rate magnitude, including zero. The latter solution method introduces two additional new tensorial fields and solve the whole problem as the minimization of a functional with a step descent Uzawa algorithm. While the regularization approach was very popular in the 80s and 90s, the community has been progressively acknowledging over the past 10 years that, although solving a slightly different problem (the regularized problem) might be fine in some flow configurations, it also leads to some questions about the relevance of the computed solution, in particular in terms of the location of *yield surfaces* and the modeling of the finite time decay property. While the augmented Lagrangian algorithm and its variants solve the actual yield stress model, their main drawback is their prohibitive computational cost related to a rather slow convergence rate. New active research directions over the second decade of the 21st century aim at developing algorithms for solving the initial, unregularized, problem but with a faster convergence rate and lower computing time. This will open up new perspectives in the numerical simulation of yield stress fluid flows, in particular it might eventually make simulation of three-dimensional flows possible.

Section 1 presents the viscoplastic flow problem and its mathematical statement. Section 2 reviews the two main algorithmic approaches: (i) regularization approach and (ii) augmented Lagrangian algorithm. This section closes by a review of recent strategies for fast-and-accurate algorithms. Section 3 presents common extensions of the conventional viscoplastic Bingham and Herschel-Bulkley models: yield slip at the wall, non-constant coefficients (granular materials, mixtures, thermal effects or thixotropy), elasticity and shallow flow reduced models.

1 Problem statement

The total Cauchy stress tensor of a viscoplastic fluid is expressed by $\boldsymbol{\sigma}_{tot} = -p\,I + \boldsymbol{\sigma}$ where $\boldsymbol{\sigma}$ denotes its deviatoric part, and p is the pressure. The constitutive equation for a viscoplastic fluid writes:

$$\begin{aligned} &\boldsymbol{\sigma} = 2K\,|2D(\boldsymbol{u})|^{n-1}D(\boldsymbol{u}) + \sigma_0\frac{D(\boldsymbol{u})}{|D(\boldsymbol{u})|} && \text{if } |D(\boldsymbol{u})| \neq 0 \\ &|\boldsymbol{\sigma}| \leqslant \sigma_0 && \text{if } |D(\boldsymbol{u})| = 0 \end{aligned} \tag{1}$$

where $\sigma_0 \geqslant 0$ is the yield stress, $K > 0$ is the consistency, $n > 0$ is the power-law index, $\boldsymbol{u}$ is the velocity field, $D(\boldsymbol{u}) = (\nabla\boldsymbol{u} + \nabla\boldsymbol{u}^T)/2$ is the rate-of-deformation tensor, and, for any tensor $\tau = (\tau_{ij})$, the notation $|\tau|$ represents the following matrix norm:

$$|\tau| = \sqrt{\frac{\tau:\tau}{2}} = \left(\frac{1}{2}\sum_{ij}\tau_{ij}^2\right)^{\frac{1}{2}}$$

The $1/2$ factor under the square root is only a convenient convention: for a simple shear flow, $\dot\gamma = |2D(\boldsymbol{u})|$ coincides with the absolute value of the shear rate, otherwise it would be counted twice. Note that when $\sigma_0 = 0$ and $n = 1$, the model (1) reduces to the classical viscous incompressible fluid. When $\sigma_0 \geqslant 0$ and $n = 1$, we obtain the tridimensional extension of the Bingham model, as formulated by Oldroyd [132]. In the general case $\sigma_0 \geqslant 0$ and $n > 0$, we obtain the tridimensional extension of the Hershel-Bulkley model [93]. Note also that tacking the norm of (1) leads to a simple scalar relation, suitable for simple shear flows:

$$|\boldsymbol{\sigma}| = K\,\dot\gamma^n + \sigma_0$$

The conservation of momentum expresses:

$$\rho\left(\frac{\partial\boldsymbol{u}}{\partial t} + (\boldsymbol{u}.\nabla)\boldsymbol{u}\right) - \mathbf{div}\,\boldsymbol{\sigma} + \nabla p = \boldsymbol{f} \tag{2}$$

where $\boldsymbol{f}$ denotes the external forces (e.g. the gravity) and ρ is the constant density. Thus, the mass conservation leads to:

$$\operatorname{div}\boldsymbol{u} = 0 \tag{3}$$

The set of equations (1)-(3) is closed by some appropriate initial and boundary conditions and the problem is complete.

Note that the viscoplastic fluid is characterized by the following property: the material starts to flow only if the applied forces exceed the yield stress σ_0. When $\sigma_0 > 0$, one can observe *unyielded regions* in the interior of the fluid, where $D(\boldsymbol{u}) = 0$, i.e. where the material behaves as a solid. When σ_0 increases, these unyielded regions develop.

The mathematical analysis of this problem is an ongoing work. In 1965, Mosolov and Miasnikov [120,121,122] considered a variational formulation of the problem for a Poiseuille flow with a general non-circular cross section and studied qualitative properties of it. Existence and uniqueness of the solution and the structure of the flow were investigated, especially the shape of yield surfaces. In 1976, Duvaut and Lions [68] also provided a theoretical analysis for Poiseuille flows and flows in a reservoir. These authors investigated existence, uniqueness and regularity of the solution for steady and non-stationary flows. Existence and extra regularity results on the problem with Dirichlet boundary conditions for a driven cavity flow was also studied by Fuchs and Seregin [79,80,81] (see also [82, chap. 3]). The expected regularity of the solution of the Bingham problem is still an open question, but it seems unreasonable to hope for a high regularity: in specific cases, such as Poiseuille or Couette flows, the velocity is known to have a limited regularity across the yield surface, separating yielded and unyielded regions.

2 Algorithms for viscoplastic models

This section starts with an historical overview, followed by a review of the two main solution methods available in the literature: the regularization approach and the augmented Lagrangian algorithm. A review of other recent methods completes this section.

2.1 Overview

The first numerical resolution was performed in 1972 by Fortin [75] for a flow in a pipe with a square section, based on a nonlinear relaxation method. The augmented Lagrangian algorithm has been introduced in 1969 by Hestenes [94] and Powell [138]. During the 1970s, this algorithm became popular for solving optimization problems (see e.g. Rockafellar [143]). In 1980, Glowinski [84] and then Fortin and Glowinski [76] proposed to apply it to the solution of the linear Stokes problem and also to other non-linear problems, including Bingham fluid flows. In 1980, Bercovier and Engelman [22] proposed a

regularization approach by introducing a viscosity function. In 1987, another viscosity function was proposed by Papanastasiou [136]. During the 1980s and the 1990s, numerical computations for Bingham flow problems were dominated by the regularization approach, perhaps due to its simplicity, while the augmented Lagrangian algorithm did not supply yet convincing results for practical viscoplastic flow applications. In 1989, Glowinski and le Tallec [85] revisited the augmented Lagrangian algorithm, using new optimization and convex analysis tools, such as subdifferential, but no evidence of the efficiency of this approach to viscoplasticity was showed, while regularization methods became more popular in the 1990s with the work of Mitsoulis *et al* [115] and Wilson and Taylor [183]. In 2001, Saramito and Roquet [153,144] showed for the first time the efficiency of the augmented Lagrangian algorithm, especially when combined with an auto-adaptive mesh technique for capturing accurately yield surfaces, across which the solution looses some regularity. In the 2000s, this approach became mature and a healthy competition developed between the regularization approach and the augmented Lagrangian algorithm. In 2003, Vola, Boscardin and Latché [179] obtained results for a driven cavity flow with the augmented Lagrangian algorithm while Mitsoulis *et al* [116] presented computations for an expansion flow with the regularization approach. In a series of papers, Frigaard *et al* [123, 78,141] pointed out some drawbacks of the regularization approach. Finally, at the end of the 2000s decade, the augmented Lagrangian algorithm became the most popular way to solve viscoplastic flow problems [127,61] because of its accuracy, despite the fact that the regularization approach runs in general faster. The `Rheolef` library, a free software developed by one of the authors of this review article and supporting both the augmented Lagrangian algorithm and an auto-adaptive mesh technique, is now widely used for various flow applications (see e.g. [140,146,181,34]).

2.2 The regularization approach

The main idea of the regularization approach is to modify the problem in order to recover standard equations. Let $\varepsilon \geqslant 0$ and set

$$\boldsymbol{\sigma}_\varepsilon = 2\left(K|2D(\boldsymbol{u})|^{n-1} + \frac{\sigma_0}{(|2D(\boldsymbol{u})|^2+\varepsilon^2)^{\frac{1}{2}}}\right) D(\boldsymbol{u})$$

where ε is the regularization parameter. When $\varepsilon = 0$, we recover the previous constitutive equation when $D(\boldsymbol{u}) \neq 0$. When $\varepsilon > 0$, the previous relation is well-defined, even when $D(\boldsymbol{u}) = 0$. Next, let us define the following viscosity function, proposed by Bercovier and Engelman [22]:

$$\eta_\varepsilon(\xi) = K\xi^{\frac{n-1}{2}} + \frac{\sigma_0}{(\xi+\varepsilon^2)^{\frac{1}{2}}},\ \forall \xi \in \mathbb{R}^+$$

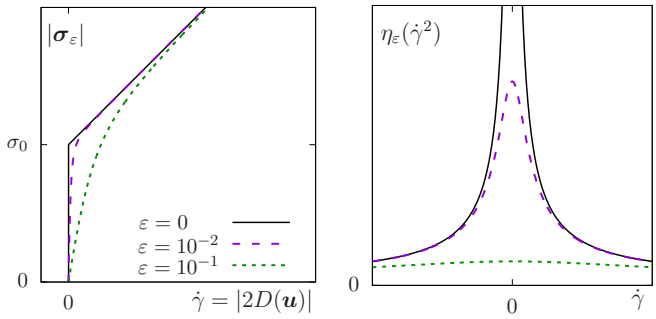

Figure 1 Regularization for viscoplastic fluids: (left) the stress ; (right) the viscosity.

Others variants of the viscosity function has been proposed: see e.g. Papanastasiou [136], Reyes and González Andrade [56] and also [78] for a review and comparison of them. With this notation, the previous relation writes:

$$\boldsymbol{\sigma}_\varepsilon = 2\eta_\varepsilon\left(|2D(\boldsymbol{u})|^2\right) D(\boldsymbol{u}) \tag{4}$$

When $\varepsilon > 0$, the fluid is a quasi-Newtonian one. By this way, there is no more division by zero when $D(\boldsymbol{u}) = 0$ and we know efficient algorithms to solve such quasi-Newtonian fluid flow problems (see e.g. [151, chap. 2]). Fig. 1 plots the stress and the viscosity function versus the shear rate. Replacing the expression (4) of the stress in (2), we obtain, together with (3), a variant of the incompressible Navier-Stokes equations with a non-constant viscosity: this problem can be easily implemented by using any existing softwares dedicated to the solution of the Navier-Stokes equations.

The simplest way to solve the nonlinear set of equations is the Picard fixed point method (see e.g. [1]). For instance, combined with a Chorin pressure projection algorithm to deal with the incompressibility constraint and with a staggered finite difference discretization scheme, we obtain a popular approach, the so-called SIMPLE method, that is widely used in computational fluid dynamics and has been used for viscoplastic fluid flows by Syrakos *et al* [162]. A more sophisticated way is the Newton method, that offers the advantage of a quadratic convergence rate of the residual terms. It was also investigated by several authors [26,160,56,8]. These two nonlinear methods lead to a succession of linear system with a very bad condition number (the ratio of the largest eigenvalue to the smallest eigenvalue), due the large variations of the apparent viscosity η_ε. For bidimensional geometries or small to medium meshes, this linear system could be solved by a direct solver, while iterative solvers are required for large or tridimensional meshes. This last issue, and related preconditioning techniques, has been explored recently by Grinevich and Olshanskii [91] and by Aposporidis *et al* [8,9].

A first weakness of the regularization approach is the lack of general convergence results of the solution with ε, denoted as $(\boldsymbol{\sigma}_\varepsilon, \boldsymbol{u}_\varepsilon)$ of the regularized problem to the

original solution $(\boldsymbol{\sigma}, \boldsymbol{u})$ when $\varepsilon \longrightarrow 0$. In [86, p. 370] there is a convergence result for the velocity field $\boldsymbol{u}_\varepsilon$, in the case of the Bingham model ($n = 1$) and for the one-dimensional Poiseuille flow where the domain of computation Ω is a circular pipe section (see [188] for some generalizations). There is no convergence results available concerning the corresponding stress deviator $\boldsymbol{\sigma}_\varepsilon$ and, from numerical experiences, there is no evidence that this quantity converges to the solution $\boldsymbol{\sigma}$ associated to the unregularized problem [78,141]: the velocity vector converged while decreasing ε whereas no convergence of the stress tensor is observed. Recall that the computation of the stress tensor is crucial for the determination of unyielded regions, characterized by $\{\boldsymbol{x} \in \Omega,\ |\boldsymbol{\sigma}_\varepsilon(\boldsymbol{x})| < \sigma_0\}$. Thus, we need a point-wise convergence of $\boldsymbol{\sigma}_\varepsilon$ to $\boldsymbol{\sigma}$ when ε tends to zero. Finally, regularized models may lead to an inaccurate prediction of unyielded regions. From (4), observe that $\boldsymbol{\sigma}_\varepsilon$ involves a product of η_ε and $D(\boldsymbol{u}_\varepsilon)$. There is an issue in unyielded regions, where the fluid is in rigid motion, i.e. where $D(\boldsymbol{u}_\varepsilon)$ tends to zero with ε. Recall that the velocity and its gradient are convergent with ε. In that case, as the viscosity η_ε involves a division by $|D(\boldsymbol{u}_\varepsilon)|$, this viscosity tends to infinity, their product in the expression of $\boldsymbol{\sigma}_\varepsilon$ appears as indeterminate and there is no evidence that this product tends here to some finite value.

A second weakness of this approach is the disappearance of unyielded regions when tracked as $D(\boldsymbol{u}) = 0$. For instance, when solving the Poiseuille flow problem with this modified model, the velocity is not constant anymore at the center of the pipe. For the Couette flow, there is no motionless unyielded region anymore and the position of the yielded surface is difficult to determine. Finally, with this modified problem, return to rest in finite time and *quiescent state* [127] cannot be captured: the flow never fully stops when the load is lower than the critical value. The finite time decay, quiescent state and limit load analysis can not be established clearly. The prediction of stability of building foundations in civil engineering or mechanical robustness of engine parts becomes thus problematic. Also when trying to predict natural hazards, such as landslides, mud flows, snow avalanches or volcanic lava flows, the disastrous event is always predicted, as the material can never be at the rest on a slope under gravity forces. Nevertheless, this approach remains simple to implement in existing codes [115,166,129] and also useful when computations do not aim at predicting accurately either unyielded regions or a quiescent state. See also the review [117] in the present journal volume for some applications of the regularization approach. The next paragraph presents an alternative approach that is able to address accurately both unyielded regions and finite time decay to a quiescent state.

2.3 The Augmented Lagrangian algorithm

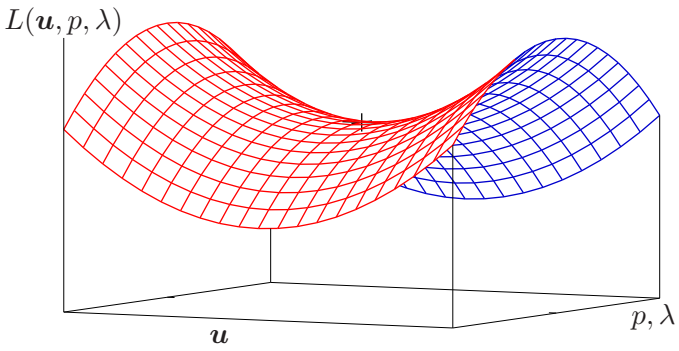

Figure 2 Saddle-point problem formulation of a viscoplastic fluid flow.

In this paragraph, we consider a steady problem and the inertia term $(\boldsymbol{u}.\nabla)\boldsymbol{u}$ is also neglected. It is a common assumption, as many viscoplastic flows are slow. Here, this assumption is done without loss of generality: the inertia term can be reintroduced, e.g. as a right-hand side in a time-dependent algorithm, and at each time step, there is a stationary problem to solve, as considered in this paragraph. See e.g. [182,105] for such a simple explicit treatment of the inertia term, and [59,126] for a more elaborated decoupled scheme.

The stationary and inertialess viscoplastic problem can be equivalently rewritten as the minimization of the viscous energy J defined by:

$$J(\boldsymbol{u}) = \int_\Omega \frac{K}{1+n} |2D(\boldsymbol{u})|^{1+n} \,\mathrm{d}x + \int_\Omega \sigma_0 |2D(\boldsymbol{u})| \,\mathrm{d}x - \int_\Omega \boldsymbol{f}.\boldsymbol{u} \,\mathrm{d}x$$

under the velocity divergence-free constraint and boundary conditions. Pressure represents as usual the Lagrange multiplier associated to the velocity divergence-free constraint. Here, a new independent variable $\boldsymbol{\delta}$, satisfying $\boldsymbol{\delta} = 2D(\boldsymbol{u})$, is introduced. The relation $\boldsymbol{\delta} = 2D(\boldsymbol{u})$ is treated as a new constraint and is imposed with a second Lagrange multiplier denoted as $\boldsymbol{\sigma}$. This notation is coherent, as $\boldsymbol{\sigma}$ coincides with the stress deviator. The situation is as follows:

constraint	Lagrange multiplier
$\operatorname{div} \boldsymbol{u} = 0$	p
$\boldsymbol{\delta} = 2D(\boldsymbol{u})$	$\boldsymbol{\sigma}$

The Lagrangian functional is defined by:

$$L\left((\boldsymbol{u}, \boldsymbol{\delta}),\ (p, \boldsymbol{\sigma})\right) = \int_\Omega \frac{K}{1+n} |\boldsymbol{\delta}|^{1+n} \,\mathrm{d}x + \int_\Omega \sigma_0 |\boldsymbol{\delta}| \,\mathrm{d}x - \int_\Omega \boldsymbol{f}.\boldsymbol{u} \,\mathrm{d}x - \int_\Omega p \operatorname{div} \boldsymbol{u} \,\mathrm{d}x + \frac{1}{2} \int_\Omega \boldsymbol{\sigma} : (2D(\boldsymbol{u}) - \boldsymbol{\delta}) \,\mathrm{d}x + \frac{r}{2} \int_\Omega |2D(\boldsymbol{u}) - \boldsymbol{\delta}|^2 \,\mathrm{d}x$$

Here, $r \geqslant 0$ is an augmentation parameter and when $r \neq 0$ the Lagrangian is called the augmented Lagrangian. Then, the corresponding saddle-point problem is equivalent to the previous minimization problem. It is solved by a specific constant step descent algorithm (Uzawa) with respect to the stress $\boldsymbol{\sigma}$: this is the so-called augmented Lagrangian algorithm. See e.g. [151, chap. 3] for a recent and detailed presentation of this algorithm.

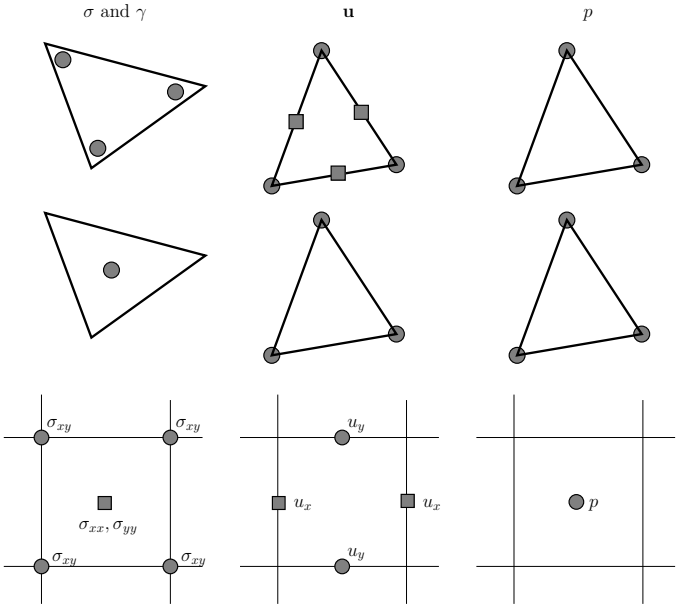

Figure 3 Some commonly used discretizations for the stress-velocity-pressure mixed formulation. From top to bottom: $P_{1,disc}$–P_2–P_1 and P_0–P_1–P_1 finite elements ; staggered finite difference scheme.

There is mainly two methods in use for the discretization of the continuous problem: the finite element and the finite difference methods (see Fig. 3). Mixed finite elements were proposed by Roquet and Saramito [144] with the Taylor-Hood P_2–P_1 approximation for the velocity-pressure pair and linear discontinuous approximation of the tensor variables (see also [146,34]). Stabilized mixed finite elements was used by Vola *et al* [179,110] with the stabilized mini-element P_1–P_1 for the velocity-pressure pair and piecewise constant approximation of the tensor variables (see also [186]). The finite difference (sometimes called finite volume) method was used by Vinay *et al* [177] (see also [127,87,105,185,182]) with staggered grids: components of velocities and tensor components are not located at the same grid position, as shown on Fig. 3. Recently, Muravleva and Olshanskii [125,134] explored a non-staggered finite difference scheme, where all velocity and stress components are located at the same grid position.

The first advantage of the augmented Lagrangian algorithm is its ability to compute an accurate prediction of yield surfaces, especially when combined with mesh adaptation [153,144] (see also Fig. 4). This combination is now used for practical applications (see e.g. [180, 147]). Also, the quiescent state (limit load analysis) is well-predicted [153,127,181]. Second advantage, the algorithm reduces simply to a succession of Stokes-like subproblems with constant viscosity coefficients: these subproblems are easier to solve than the subproblems of the regularized approach, with very high viscosity variations.

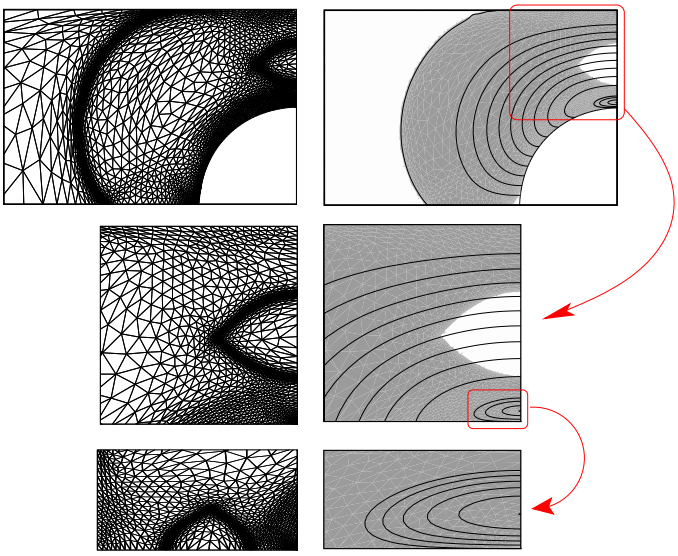

Figure 4 Flow of a viscoplastic fluid around a moving cylinder: zoom on the adaptive mesh (from [144]).

The main drawback of the augmented Lagrangian algorithm is the computing time required to obtain the solution: the next paragraph reviews some alternative approaches for solving more efficiently the unregularized viscoplastic problem.

2.4 Others unregularized approaches

While the regularization approach is relatively fast, at least when solved by a Newton algorithm, the accurate prediction of yielded surfaces could be problematic [78, 61]. Conversely, the augmented Lagrangian algorithm is able to predict accurately the location of yield surfaces [144] but its computing time is generally larger. Except the augmented Lagrangian algorithm, in the 20th century, few unregularized approaches were known [23, 163] and were only valid for a very limited range of applications. Recently, several attempts have been proposed to design *fast and accurate* algorithms for the resolution of the *unregularized* viscoplastic problem.

In 2010, Reyes and González Andrade [54,55] proposed a semi-smooth Newton algorithm combined with a Tikhonov regularization of the problem. Nevertheless, a few years later [56, p. 44], this approach has been found

to be equivalent to a new variant of the regularization approach, as presented in section 2.2. The existence of commercial libraries dedicated to large optimization problems has been explored in 2015 by Bleyer *et al* [30]. The authors claimed that their approach "*does not require any regularization of the viscoplastic model*", despite the fact that the used commercial library is based internally on an interior point method, i.e. a Newton method on a regularized problem combined with a continuation on the regularization parameter (see e.g. [35, chap. 11]). Finally, the point-wise convergence of the stress tensor and the related accuracy of unyielded regions predicted by this approach have not yet been addressed.

In 2014, Aposporidis *et al* [9] proposed a Picard fixed point algorithm for a new reformulation of the unregularized viscoplastic problem. At each iteration, the linear system is solved by an iterative solver and the solver is accelerated by an efficient preconditioning technique based on a regularization of the reformulated problem. In 2015, Chupin and Dubois [47] proposed a Chorin-like projection scheme combined with a Picard fixed point algorithm. In 2015, Treskatis *et al* explored an acceleration of the augmented Lagrangian algorithm [168] based on the fast iterative shrinkage-thresholding algorithm (FISTA).

One of the most efficient algorithms to solve nonlinear problems is the Newton method, due to its super-linear convergence properties. Applying the Newton method to the unregularized viscoplastic problem leads to a singular Jacobian matrix. This difficulty has been recently addressed by using the trusted region algorithm [167], that regularizes the Jacobian matrix but loses the superlinear convergence of the method. In 2016, Saramito [152] addressed directly the singularity of the Jacobian matrix in the Newton method in order to preserve the superlinear convergence. Fig. 5 plots the residue of the equations versus the computing time: observe the spectacular improvement of convergence for the solution of an unregularized viscoplastic problem.

Table 1 summarizes these various recent approaches and compares them in terms of their asymptotic convergence rate: there is actually three classes of algorithms for the unregularized problem. The more classical approach, the augmented Lagrangian, shows a polynomial convergence rate of the residual term $r_n \approx n^{-\alpha}$ where n is the iteration number and α is a constant. Plotting r versus n in log-log scale, as on Fig. 5, shows an asymptote with slope $\alpha \approx 0.9$. The FISTA acceleration [168] replaces α by 2α while the convergence remains polynomial. Both Picard fixed point [9] and trust-region [167] methods improve this asymptotic convergence as $r_n = \exp(-\alpha n)$. The most efficient algorithm is certainly the Newton one [152] with a quadratic convergence $r_n = \alpha\,(r_{n-1})^2$ (see also Fig. 5).

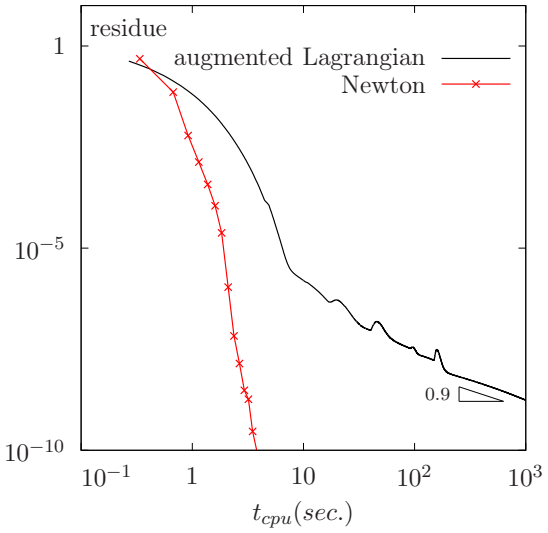

Figure 5 Comparison between the Newton method and the augmented Lagrangian algorithm (AL) for the Herschel-Bulkley viscoplastic problem (from [152]).

3 Extensions of the model

This section reviews various extensions of the conventional viscoplastic Bingham and Herschel-Bulkley models. Many viscoplastic fluids slips at the wall with a yield slip and corresponding slip models share some analogies with yield stress models (paragraph 3.1). Models with non-constant yield stress and consistency coefficients that depend on shear rate and pressure are commonly used for granular models (paragraph 3.2). Thixotropy (paragraph 3.3) suppose also a dependence of these coefficients on a material field, thermal effects (paragraph 3.4) introduce a dependence on temperature, while mixtures use a dependence on volume fraction (paragraph 3.5). Tacking into account the elasticity of the material leads to elastoviscoplastic models (paragraph 3.6). Finally, Shallow-flow approximations are commonly used for environmental and industrial applications when the vertical/horizontal aspect ratio of the flow is small (paragraph 3.7).

3.1 Yield slip boundary conditions

Slip occurs in the flow of two-phase systems, such as polymer solutions, emulsions, and particle suspensions, because of the displacement of the disperse phase away from solid boundaries. There is, close to the wall, a thin layer of fluid of lower viscosity than that of the bulk material, so that the shear amplitude is much larger in this layer than in the rest of the flow domain. This phenomenon appears to be more pronounced when the material possesses a yield stress, such as pastes. In practical viscoplastic flow problems such as concrete pumping, it

efficiency	convergence	rate	methods and contributors
slow	power-law	$r_n = n^{-\alpha}$	augmented Lagrangian [144] ; FISTA [168]
medium	linear	$r_n = \exp(-\alpha n)$	Picard fixed point [9] ; trust-region [167]
fast	quadratic	$r_n = \alpha\,(r_{n-1})^2$	Newton [152]

Table 1 What is fast and slow ? Asymptotic convergence of various unregularized algorithms.

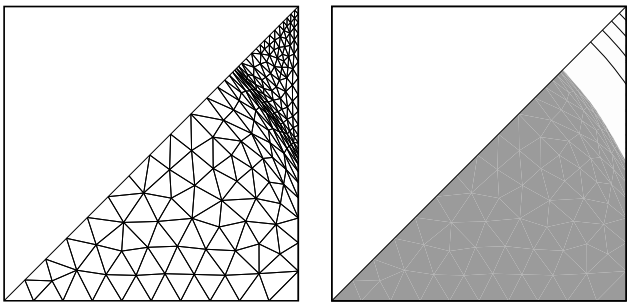

Figure 6 Slip at the wall for a pipe flow of a Bingham fluid with a square section (from [145]).

also seems that a no-slip boundary condition is not a satisfactory model. The fluid slips when the tangential stress exceeds a critical value σ_s, called the yield slip, and, otherwise the fluid sticks to the wall. This critical value may be considered as an intrinsic characteristic of the material and its relation to the wall. The slip boundary condition at the wall reads:

$$\begin{aligned} \boldsymbol{u}.\boldsymbol{n} &= 0 \\ \boldsymbol{\sigma_{nt}} &= -c_f \boldsymbol{u_t} - \sigma_s \frac{\boldsymbol{u_t}}{|\boldsymbol{u_t}|} \quad \text{when } \boldsymbol{u_t} \neq 0 \\ |\boldsymbol{\sigma_{nt}}| &\leqslant \sigma_s \qquad\qquad\quad \text{when } \boldsymbol{u_t} = 0 \end{aligned}$$

where $\boldsymbol{u_t} = \boldsymbol{u} - \boldsymbol{u}.\boldsymbol{n}$ denotes the tangential velocity, $\boldsymbol{\sigma_{nt}} = \boldsymbol{\sigma n} - \sigma_{nn}.\boldsymbol{n}$ is the shear stress, $\sigma_{nn} = (\boldsymbol{\sigma n}).\boldsymbol{n}$ the normal stress, $\boldsymbol{n}$ the outward unit normal at the wall, and $c_f > 0$ is a friction coefficient. We observe that for $\sigma_s = 0$, we obtain the classical linear slip boundary condition: the fluid slips for any non-vanishing shear stress. For $\sigma_s > 0$, boundary parts where the fluid sticks can be observed. As σ_s becomes larger, these stick regions develop.

Observe the analogy between the yield slip equation and the yield stress fluid constitutive equation (1). This analogy has been exploited in 1991 by A. Fortin *et al* [74], who proposed an augmented Lagrangian algorithm for yield slip at the wall. In 2008, Roquet and Saramito [145] applied a similar approach to the Poiseuille flow of a viscoplastic fluid with a square cross section (see Fig. 6). Five flow regimes were identified in a master curve: full slip, full stick, partial slip and stick at the wall, block translation and stopped material.

In 2014, Damianou *et al* [51] investigated the time-dependent problem and the stopping time for a Poiseuille flow with a circular [51] or square [50] cross section with yield slip at the wall by using the regularization approach for both the viscoplastic model and the yield slip equation [49].

3.2 Models for dense granular material

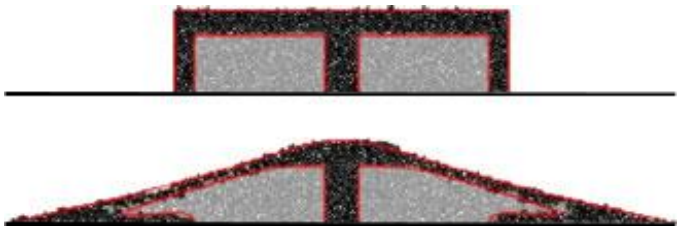

Figure 7 Comparison between the $\mu(I)$ continuum model (red line) and contact dynamics simulations (grains) for a column collapse (initial and final state). The grains are colored in the initial heap, which allows one to track the displacement (from [108]).

Early concepts to explain the behavior of granular flows were introduced in 1954 by Bagnold [11], who identified many of the features of granular media. At the beginning of the 20th century, from the collective work of the French research group *GDR milieux divisés* [114,104], emerged for the first time a constitutive equation for the flow of dense dry granular materials, considered as a liquid. The deviatoric part $\boldsymbol{\sigma}$ of the Cauchy stress tensor is expressed by

$$\boldsymbol{\sigma} = 2\ \eta_{\text{app}}(p, |2D(\boldsymbol{u})|)\ D(\boldsymbol{u})$$

where the apparent viscosity η_{app} depends on the pressure p and the shear rate $\dot\gamma = |2D(\boldsymbol{u})|$ as

$$\eta_{\text{app}}(p, \dot\gamma) = \frac{\mu(I)\,p}{\dot\gamma},\ \ \mu(I) = \frac{\mu_s I_0 + \mu_d I}{I_0 + I} \quad \text{and} \quad I = \frac{d\,\dot\gamma}{\sqrt{p/\rho}}$$

The inertial number I represents the square root of the Savage [154] or Coulomb [7] number while I_0 is a dimensionless number, d is the grain diameter and $\mu_d \geqslant \mu_s$ are frictions parameters for large and small I, respectively. This constitutive equation, often called $\mu(I)$-rheology, extended previous ideas introduced by Savage and Hutter [154,155] and Ancey *et al* [7]. The $\mu(I)$-rheology, was first used in numerical simulations in 2011 by Lagrée *et al* [108]: these authors compared the solution with results of two-dimensional contact dynamics discrete simulations for the granular column collapse benchmark (see

Fig. 7) and concluded that the constitutive equation is able to describe accurately the collapse for a large range of aspect ratios of the column. The unbounded apparent viscosity when $D(\boldsymbol{u})$ tends to zero was treated by bounding it numerically and the whole system was solved by a Chorin's like decoupled projection algorithm. Chauchat and Médale [39,40] proposed a regularization approach, inspired by those of Bercovier and Engelman [22] for the Bingham model, and then solved the whole system by a Newton algorithm. Following Bleyer *et al* [30], Daviet and Bertails-Descoubes [53], for solving the $\mu(I)$ model, used recently the interior point algorithm (i.e. a Newton method for a regularized problem combined with a continuation on the regularization parameter, see [35, chap. 11] and comments section 2.4). In 2015, Ionescu *et al* [103] addressed for the first time the unregularized $\mu(I)$ model and proposed an augmented Lagrangian algorithm, extending those presented in [144] for the Bingham model. These authors observed that the $\mu(I)$-rheology coincides with an extension of the Bingham model (1) with non-constant viscosity and yield stress coefficients:

$$\begin{aligned} &\boldsymbol{\sigma} = 2\,\eta(p,|2D(\boldsymbol{u})|)\,D(\boldsymbol{u}) + \sigma_0(p)\frac{2D(\boldsymbol{u})}{|2D(\boldsymbol{u})|} && \text{if } |D(\boldsymbol{u})| \neq 0 \\ &|\boldsymbol{\sigma}| \leqslant \sigma_0(p) && \text{if } |D(\boldsymbol{u})| = 0 \end{aligned}$$

with

$$\sigma_0(p) = \mu_s p \quad \text{and} \quad \eta(p,\dot\gamma) = \frac{(\mu_d-\mu_s)p}{\dfrac{I_0\sqrt{p}}{d\sqrt{\rho}} + \dot\gamma}$$

Note that a simplified pressure-dependent (Coulomb-like) yield stress model is the Drucker-Prager model [64]:

$$\sigma_0(p) = \overline{\sigma}_0 + \mu_s p \quad \text{and} \quad \eta(p,\dot\gamma) = \overline{\eta}_0$$

where $\overline{\sigma}_0$ and $\overline{\eta}_0$ are constants. Ionescu *et al* [103] found that the $\mu(I)$-rheology and Drucker-Prager models give very similar results for the granular column collapse benchmark. Simultaneously, in 2015, Barker *et al* [16] showed that the $\mu(I)$ model could be mathematically ill-posed in some cases and then could develop Hadamard instabilities. In 2016, these authors proposed a well-posed variant [17]:

$$\mu(I) = \frac{\mu_s I_0 + \mu_d I + \alpha I^2}{I_0 + I}$$

where $\alpha > 0$ is a stabilization parameter.

3.3 Thixotropy

The literature on thixotropic materials is extremely vast, but every thixotropic material is not necessarily a viscoplastic material and some of them are purely viscous. Cement slurries, drilling muds, cosmetics and personal care products, waxy crude oils, fire fighting foams are among many examples of thixotropic viscoplastic materials. Viscoplasticity is often related to a particular micro-structure of the material: jamming, colloidal forces, soft chemical bonds, fibers orientation, etc. This micro-structure evolves over short times to breakdown when the material is subjected to a certain stress or strain load [45,88,18,124,48,135]. Conversely, it evolves over long times to recovery when left to rest. This micro-structure is generally described by a scalar field, denoted λ, that indicates the level of structuring of the material [97,57,58]. A zero value represents a fully broken down material and a value of 1 or $+\infty$, depending on the model, represents a fully structured material. In the vast majority of models, the yield stress σ_0 is a function of the field λ and hence evolves with time and stress or strain rate.

In the late 50s, Moore [119] suggested an unsteady advection-reaction equation for the structure field λ, that covers a wide range of thixotropic materials. Moore depicted the material micro-structure as composed of a number of links with the rheological behavior of the material a function of the number of links formed. Moore interpreted the structure field λ as the ratio of formed links to the total number of potential links. Hence when $\lambda = 0$, all links are destroyed and when $\lambda = 1$ all links are formed. In the popular Houska model [97] (see also [60, 182,87]), the reaction term comprises a shear rate dependent breakdown term and a recovery term:

$$\frac{\partial\lambda}{\partial t} + \boldsymbol{u}.\nabla\lambda = a(1-\lambda) - b\lambda\dot\gamma^m$$

where λ takes its values in $[0,1]$ and $\dot\gamma$ is the generalized shear rate. Also, a, b and m are the three experimentally measurable constants of the model. Note that a has the dimension of the inverse of time, thus $1/a$ represents the time scale of recovery. In many models, recovery is associated to Brownian rearrangement of the micro-structure. Here, m is a power-law index. When $m = 1$, b represents the magnitude of shear induced structure breakdown and is dimensionless. Other models as e.g. [65,66], may include a shear induced recovery but are conceptually very similar as far as the advection-reaction equation for the structure field is concerned. Following Moore, consistency and yield stress of the material are function of the structure field λ. For instance, Houska [97] suggested a linear dependence as follows:

$$K = \bar{K}_0 + \lambda\bar{K}_1 \quad \text{and} \quad \sigma_0 = \bar{\sigma}_0 + \lambda\bar{\sigma}_1$$

where $\bar{K}_0$ and $\bar{\sigma}_0$ denote consistency and yield stress of the fully broken down material, respectively, and $\bar{K}_0 + \bar{K}_1$ and $\bar{\sigma}_0 + \bar{\sigma}_1$ denote consistency and yield stress of the fully recovered material, respectively. The Houska model contains thus seven parameters $(a, b, m, \bar{K}_0, \bar{K}_1, \bar{\sigma}_0$ and $\bar{\sigma}_1)$ that are all measurable experimentally [38,92].

Note that the main issue in solving a thixotropic viscoplastic flow problem arises from the two-way coupling of the momentum conservation equation and the constitutive equation via the λ equation: the momentum conservation with $\boldsymbol{u}$ depends on λ through K and σ_0 and λ depends on $\boldsymbol{u}$ through the advection term $\boldsymbol{u}.\nabla\lambda$ in the equation above. In 2009, Wachs *et al* [182,87] solved this coupled time-dependent set of equations by a decoupled approach, where the reaction term is treated explicitly, i.e. at the previous time step. Each time step reduces to an explicit computation for λ and a stationary viscoplastic subproblem. When the micro-structural changes do not occur too fast, this approach allows large time steps, otherwise the time step should be decreased as the scheme is conditionally stable. When solving the stationary viscoplastic subproblem with an augmented Lagrangian algorithm, it is conceivable to also update λ during iterations without loosing the usual robust convergence properties. In 2011, Negrão *et al* solved this coupling by a combination of semi-explicitness and Newton algorithm [128].

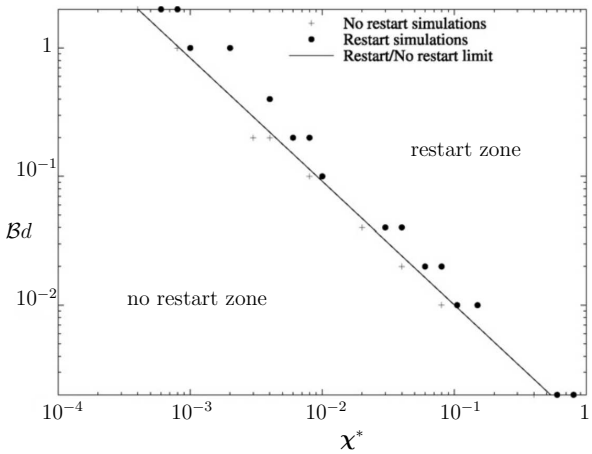

Figure 8 Combined effects of thixotropy and compressibility for the restart of the weakly compressible flow in a pipeline filled with a viscoplastic and thixotropic material (from [182]). The Bingham number is set to a value larger than the classical restart limit. χ^* and $\mathcal{B}d$ are dimensionless numbers for compressibility and thixotropy, respectively.

Among the various flow configurations of interest to the viscoplastic community, the start up flow of a thixotropic and viscoplastic material in a pipe has received a significant attention (see [158,37,182,87,128,3] and the references therein). In fact, it is representative of the industrial problem of restarting the flow of a waxy crude oil in a pipeline, a major and costly issue for oil and gas companies. Combined to additional weakly-compressible effects, the flow exhibits different mechanisms to restart. In particular, compressibility combined to thixotropy enable the flow to restart and recover steady flowing conditions for a pressure drop lower than the classical estimate derived from a simple force balance, a remarkable property. The ability to restart can hence be mapped in a compressibility number-thixotropy number space, as illustrated in Fig. 8 and explained in [182].

3.4 Thermal effects

Viscoplastic fluid flows with heat transfer lead to a rich variety of flow patterns and unconventional dynamics. From the early ages of viscoplastic fluid flows, researchers got interested in heat transfer for obvious practical reasons in industrial processes and flows. Some of the earliest references on an analytical work on heat transfer in Bingham fluid flows dates, to the best of our knowledge, from the late 50s [156,184,67,46]. Assuming the Boussinesq approximation $\rho = \rho_0(1-\beta(\Theta-\Theta_r))$ holds, the most general non-isothermal viscoplastic fluid flow problems reads as follows:

$$\begin{aligned}
&\boldsymbol{\sigma} = 2K(\Theta)\,|2D(\boldsymbol{u})|^{n-1}\,D(\boldsymbol{u}) \\
&\qquad\qquad +\sigma_0(\Theta)\frac{2D(\boldsymbol{u})}{|2D(\boldsymbol{u})|} \qquad \text{if } |D(\boldsymbol{u})| \neq 0 \\
&|\boldsymbol{\sigma}| \leqslant \sigma_0(\Theta) \qquad\qquad \text{if } |D(\boldsymbol{u})| = 0 \\
&\rho_0 C_p\left(\frac{\partial \boldsymbol{\Theta}}{\partial t} + (\boldsymbol{u}.\nabla)\boldsymbol{\Theta}\right) - \mathbf{div}\, k\nabla\Theta - \boldsymbol{\sigma}:D(\boldsymbol{u}) = 0 \\
&\rho_0\left(\frac{\partial \boldsymbol{u}}{\partial t} + (\boldsymbol{u}.\nabla)\boldsymbol{u}\right) - \mathbf{div}\,\boldsymbol{\sigma} + \nabla p = -\rho_0 \boldsymbol{g}\beta(\Theta-\Theta_r) \\
&\mathrm{div}\,\boldsymbol{u} = 0
\end{aligned}$$

with suitable initial and boundary conditions. Here, Θ denotes the temperature field, ρ_0 the reference density at the reference temperature Θ_r, C_p the heat capacity, k the thermal conductibility and β the thermal expansion coefficient at constant pressure.

Thermal effects as a result of significant temperature gradients manifest in a fluid flow with a growing level of complexity depending on the dependence or independence of material properties with temperature as follows:

i) consistency K, yield stress σ_0 and density ρ are independent of temperature. The heat transfer regime is forced convection. The specificity of viscoplastic heat transfer stems from the convection term in the energy equation as the convecting velocity field is a viscoplastic velocity field. Momentum and energy conservation equations are one-way coupled only [131, 31],

ii) consistency K, yield stress σ_0 and density ρ are still independent of temperature but temperature gradients develop in the flow as a result of energy dissipation [156]. This is also referred to as *viscous heating* or heat generation. This situation has not received a large attention in the literature although it should lead to interesting temperature distribution. In fact, in a yield stress fluid flow, unyielded regions, by definition, do not dissipate energy, as $D(\boldsymbol{u}) = 0$ in these regions,

iii) consistency K or yield stress σ_0 are temperature-dependent. The heat transfer regime is forced convection but now momentum and energy conservation equations are two-way coupled through the temperature dependence of the constitutive equation. In particular, the spatially variable yield stress as a function of temperature distribution can disturb the shape of yield surfaces [177,87],

iv) density ρ is temperature-dependent but this dependence is assumed to be weak such that the Boussinesq approximation is valid. The heat transfer regime is free (also called natural) convection over which an additional buoyancy term in the momentum equation drives motion [187,174,175,176,171,172,130,98,105]. Unsteady buoyancy-driven flows of a viscoplastic material can lead to a very unusual and remarkable intermittent behavior [106].

In the aforementioned papers, a decoupled semi-explicit scheme is proposed for the time-dependent problem, i.e., at t^{n+1}:

1. solve the momentum equation with $\Theta^n = \Theta(t^n)$,
2. solve the energy equation with $\boldsymbol{u}^{n+1} = \boldsymbol{u}(t^{n+1})$.

Vinay *et al* [177] proposed a fully explicit loose-coupling scheme (see also [87,105,106]) while Huilgol and Kefayati developed an operator splitting scheme [98]. The resulting schemes are conditionally stable and the time step should be chosen small enough for the scheme to converge accurately. Although this scheme is sufficient for most applications, it is possible to develop an unconditionally stable scheme. In 2010, Turan *et al* [171,172] propose a fully implicit time-dependent scheme with an inner fixed point loop. Note also that for computing the steady-state solution only, it is interesting to avoid a long time evolution of a time-dependent problem. In that case, strongly coupled schemes with an inner loop of fixed-point or Newton methods are particularly well suited.

Two problems have received a broad attention from the community: (i) heat transfer from an obstacle in a viscoplastic fluid flow [131,130,31] and (ii) natural convection in a differentially heated cavity [174,175,176,171,172,98,105,106]. The former problem is relatively simple and has been investigated mostly for steady-state flows with a regularization approach. It may however lead to intricate boundary layer problems and provides industrially valuable correlations of the Nüsselt number (dimensionless heat transfer coefficient) as a function of Reynolds and Bingham numbers. The latter problem is richer by essence and exhibits the usual unique features of a viscoplastic flow, i.e., existence of a critical Bingham B_{cr} for flow onset and finite time decay for Bingham number $B \leqslant B_{cr}$. This problem has been investigated both with a regularization method [174,175,176,171,172] and with an augmented Lagrangian algorithm [98,105,106]. These works all qualitatively agree with each other, although discrepancies exist in the definition and the value of B_{cr}. In a recent paper, Karimfali *et al* [105] determined B_{cr} from augmented Lagrangian simulations and showed that this computed value matches the analytically derived conductive limit. They also proved finite time decay and unconditional stability of the static limit, both analytically and computationally. Slightly changing the boundary conditions of the problem by heating the bottom wall locally leads to intricate intermittencies called thermal plumes for specific ranges of B and other dimensionless numbers, observed both at the experimental level [52] and at the simulation level [106], and illustrated in Fig. 9.

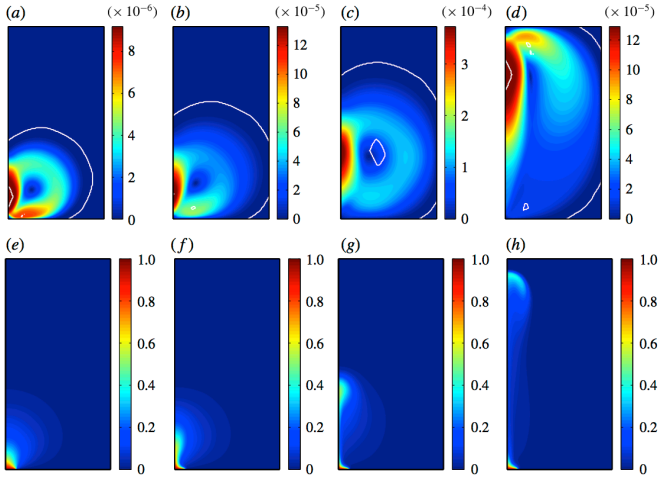

Figure 9 Thermal plumes in a locally heated natural convection flow of a Bingham fluid in a cavity (from [106]). (a-d) time evolution of dimensionless velocity magnitude and yielded surface as a white line ; (e-h) dimensionless temperature. Flow is heated from a narrow zone at the left of the bottom wall, left wall is a symmetry wall, other walls are solid walls.

Finally, very few simulation works investigated a temperature-dependent yield stress fluid flow problem and reported the effect of a spatially variable yield stress on the convergence of the selected solution algorithm (regularization or augmented Lagrangian). In [177] and Fig. 10, the convergence of the augmented Lagrangian algorithm is plotted as a function of the imposed temperature difference in the flow, which in turn indicates the amplitude of yield stress variations over the flow domain. It is quite obvious that the convergence rate is markedly affected.

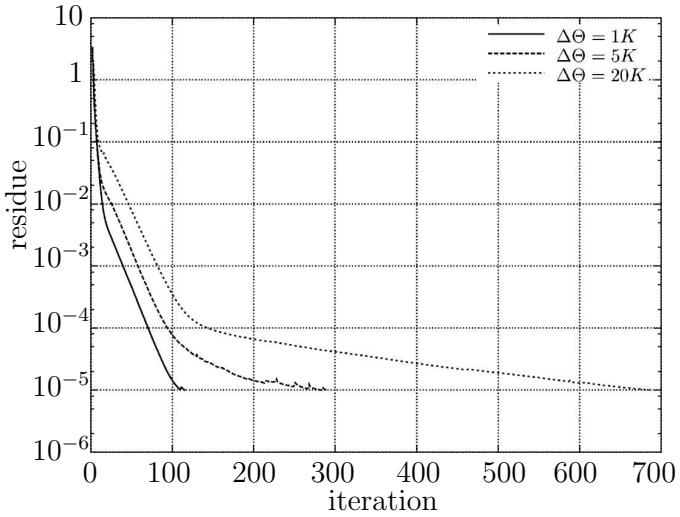

Figure 10 Convergence of the augmented Lagrangian algorithm as a function of the imposed temperature difference $\Delta\Theta$ in the flow in a temperature-dependent yield stress fluid flow in a pipeline (from [177]). The higher $\Delta\Theta$ is, the larger the amplitude of spatial variations of yield stress in the flow domain.

3.5 Two-phase flows

Many complex fluids also exhibit multiple phases, both in nature and in industry as e.g. bubbly flows, multi-layer flows and particle-laden flows. Restricting the scope to two phases only, flows of interest can be classified into two families: (i) fluid/fluid flows either liquid/liquid or gas/liquid, and (ii) fluid/solid flows. Even if the fluid phase (respectively two fluid phases) is (respectively are) Newtonian, handling the co-existence of two phases in the flow require a particular numerical treatment.

The most popular numerical modeling for fluid/fluid flows are arbitrary Lagrangian-Eulerian/mesh deforming methods [83,164,4] volume-of-fluid [95,5,96, 169,112], level set [161,159,129] or front tracking [173,178]. For fluid/solid flows there are arbitrary Lagrangian-Eulerian/mesh deforming methods [83], lattice-Boltzmann [107,139], immersed boundary [118] and fictitious domain with distributed Lagrange multiplier [185,181].

Similarly to the case of thixotropy or thermal effects, semi-implicit and decoupled scheme are deemed to be sufficient to compute solutions of satisfactory accuracy for many applications. This is probably true for flow configurations with an imposed external motion but more questionable to compute finite time decay and limit of stationary flows. In the case of suspensions and emulsions, if a force balance has to be solved for the motion of each individual droplet, bubble or particle, decoupled schemes might not be sufficient. In fact, it has been recently emphasized for the case of a single rigid particle settling in a yield stress fluid that a more sophisticated solution algorithm of the implicit or at least semi-implicit type is required to properly compute finite time decay and critical Bingham number beyond which motion is fully suppressed [181].

Multi-layer and displacement flows have received a lot of attention in the literature in relation to their broad scope of applications in industry as e.g. well drilling and cement slurry placement in oil and gas [164,5,96] or molding in polymer processing [62]. Hormozi *et al* [96] investigate the stability of multi-layer viscoplastic channel flows and establish the stability properties of the flow. They are then capable of writing stable complex shapes of Newtonian fluid injected in a Bingham channel flow and advected along the channel. Note that these computations are performed with a decoupled scheme and a volume-of-fluid method.

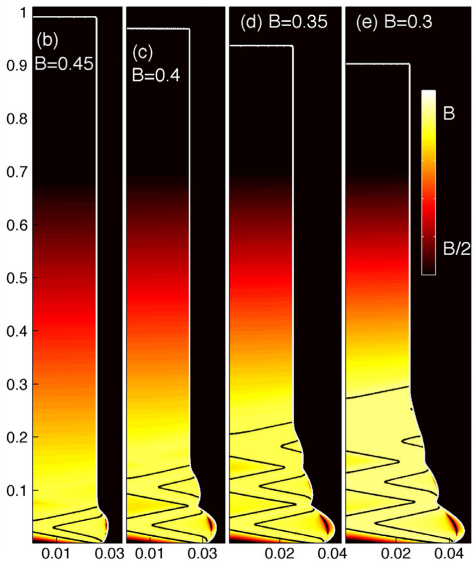

Figure 11 Original flow features characterized by free surface undulations and stress invariant zigzag pattern at the foot of a slender slumping column made of a viscoplastic material (from [112]).

A second class of problems that motivated various numerical works is free-surface flows as slumping flows (and in particular dam breaks, see also *Section 3.2*) and extrusion flows. Slumping flows are model problems relevant of a large range of geophysical applications [112] as well as industrial processes [178,4]. In dam breaks, contrary to a Newtonian fluid that should theoretically slump infinitely if surface tension is neglected, viscoplastic materials stop at a finite run-out distance. This has important implications for hazard assessment (landslides and avalanches) and industrial safety (spill of a contaminated or dangerous fluid). Both in [178] and [112], a simple decoupled scheme is deemed to perform well. Fig. 11 illustrates the original flow features unveiled by numer-

ical simulations of Liu *et al* [112] of a slender slumping column made of a viscoplastic material.

The third class of problems that has been extensively studied over the past 20 years is the gravity-driven motion of dispersed droplet/bubble or solid particle in an otherwise quiescent yield stress fluid [144,131,130,31, 159,170,139,61,169,113,181]. Actually, numerical works can be sorted into two sub-categories: (i) methods that really treat freely-moving droplet/bubble or solid particle, and (ii) methods in which the problem is formulated in the droplet/bubble/particle frame of reference or as the flow past a motionless droplet/bubble/particle. Methods of the former sub-category can be applied to single droplet/bubble/particle flows or steady multi-droplet/bubble/particle flows while methods of the latter sub-category are more general. For instance, the flow past a fixed obstacle has been extensively studied as a model problem for suspension flows [20,29, 189,144,131,130,31] and has provided some valuable insight into dimensionless drag and heat transfer coefficients and the shape of unyielded regions around the droplet/bubble/particle. The freely moving multi-droplet/bubble/particle problem has not been examined yet from a computational viewpoint, although novel results were recently published on the accurate modeling of finite time decay in the single-particle case (see FIG. 12). With the convergence rate of solution algorithms currently available to solve viscoplastic fluid flows (both regularization and augmented Lagrangian), the computing cost associated to the solution of a viscoplastic fluid flow with multiple freely moving droplets/bubbles/particles is yet too prohibitive, even on massively parallel supercomputers.

3.6 Elastoviscoplastic models

The viscoplastic constitutive equation (1) writes equivalently (see e.g. [149] or [151, chap. 5]):

$$\max\left(0, \frac{|\boldsymbol{\sigma}|-\sigma_0}{K|\boldsymbol{\sigma}|^n}\right)^{\frac{1}{n}} \boldsymbol{\sigma} = 2D(\boldsymbol{u})$$

In 2007, Saramito [149,150] proposed to take into accout the elasticity of the material with a time-dependent constitutive equation:

$$\frac{1}{G}\overset{\square}{\sigma} + \max\left(0, \frac{|\boldsymbol{\sigma}|-\sigma_0}{K|\boldsymbol{\sigma}|^n}\right)^{\frac{1}{n}} \boldsymbol{\sigma} = 2D(\boldsymbol{u}) \qquad (5)$$

where G is the elastic modulus and $\overset{\square}{\sigma}$ denotes the Gordon-Schowalters derivative [89], which is a generalization of the frame-invariant Oldroyd derivative [133] of the tensor $\boldsymbol{\sigma}$:

$$\overset{\square}{\sigma} = \frac{\partial \boldsymbol{\sigma}}{\partial t} + (\boldsymbol{u}.\nabla)\boldsymbol{\sigma} - W(\boldsymbol{u})\boldsymbol{\sigma} + \boldsymbol{\sigma}W(\boldsymbol{u}) - a\left(D(\boldsymbol{u})\boldsymbol{\sigma} + \boldsymbol{\sigma}D(\boldsymbol{u})\right)$$

where $W(\boldsymbol{u}) = (\nabla\boldsymbol{u} - \nabla\boldsymbol{u}^T)/2$ is the vorticity tensor and $a \in [-1, 1]$ is a parameter of the derivative.

This model has been first used for liquid foam by Cheddadi *et al* for Couette flows [44,43] and flows around a cylinder [42]. The set of equations is solved by a second order in time operator splitting scheme [41], the so-called θ-scheme [148], previously developed for viscoelastic fluid flow problems. Fig. 13 shows that there is very good *quantitative* agreement between calculations and experiments: the model captures quantitatively the fore-aft asymmetry and the overshoot of the velocity after the obstacle, located at $x = 0$. This overshoot of the velocity is often called the *negative wake*, in the context of a moving obstacle in a yield stress material at rest (i.e. u_x is then replaced by $-u_x$). Observe also on Fig. 13, that the Bingham model always predicts a fore-aft symmetry and no overshoot of the velocity: this is in disagreement with experimental observations on several yield stress materials such as liquid foams and carbopol solutions. Fraggedakis *et al* [77] obtained a quantitative agreement between experiments with carbopol solutions around an obstacle and numerical simulations with the elastoviscoplastic model (5): loss of the fore-aft symmetry and formation of the negative wake.

In 2010, a regularized approach for solving the elastoviscoplastic model (5) was proposed by Park and Liu [137] and results were compared to carbopol experiments for an oscillatory pipe flow. Comparisons between elasto-viscoplastic model predictions and experiments in large amplitude oscillatory shear (LAOS) were performed by McKinley *et al* [69,63]. In 2011, Belblidia *et al* [21] also combined the elastoviscoplastic model (5) with a regularization approach and performed computations in a contraction-expansion geometry. Souza-Mendes [57,58] combines both a regularized approach of viscoplasticity with elasticity and thixotropy (see section 3.3).

3.7 Shallow-flow approximations

Time-dependent three-dimensional simulations of free surface flows are motivated by industrial and environmental applications, e.g. for the numerical prediction of many natural hazards, such as avalanches, landslides, volcanic lava, mud or debris flows (see also *Section 3.2* and *Section 3.5*). Generally, there is a large ratio between the two horizontal scales and the flow height, and this would require very large meshes. The development of reduced viscoplastic models for shallow flows is a less prohibitive computational cost approach: a three-dimensional problem reduces to a two-dimensional problem and the free surface is directly handled by a height field that appears as an additional unknown in the reduced model.

For Newtonian fluids, this problem was first motivated by hydraulic engineering applications. In 1887, Barré

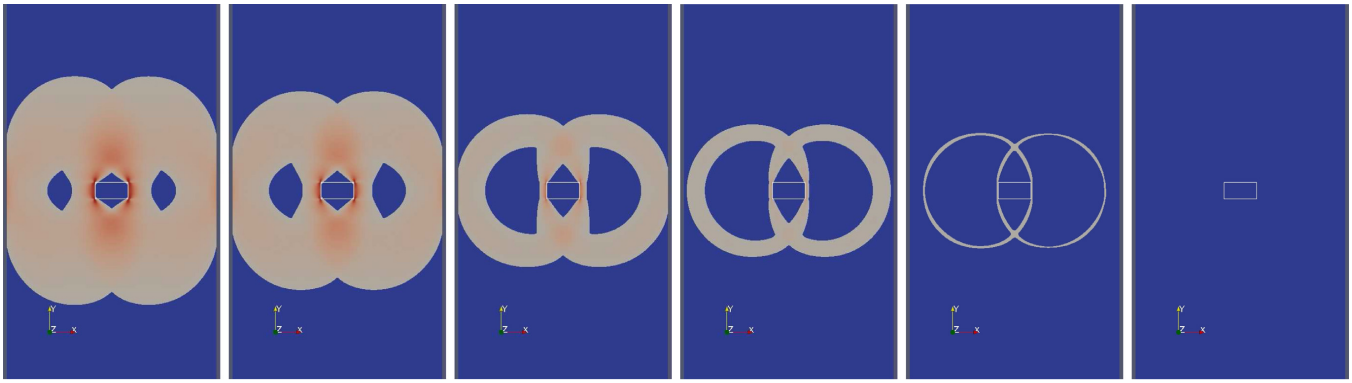

Figure 12 Return to rest in finite time for a rectangular particle settling in a viscoplastic material (from [181]). The fluid/particle system has been initially assigned a Newtonian motion and the yield stress increase abruptly from 0 to a value beyond the stationary limit. Blue regions are unyielded regions.

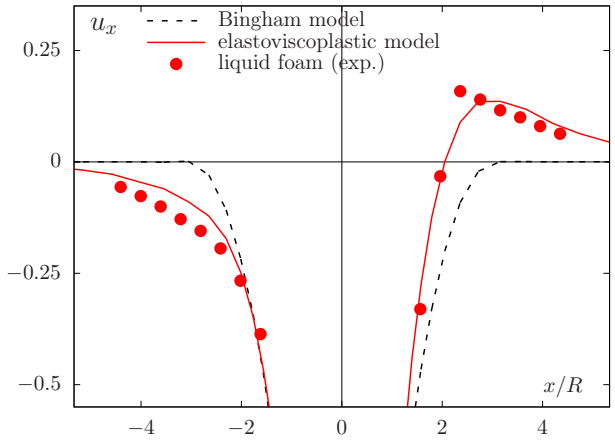

Figure 13 Flow around a circular obstacle, velocity along the axis (from [42]). Comparison between Bingham model (dashed line), elastoviscoplastic model (solid line) and liquid foam experiment (closed squares)

de Saint-Venant [19] introduced the shallow water approximation for fast Newtonian flows, driven by inertia terms while viscous effects are neglected. More recently, in 1982, Huppert [99] investigated slower Newtonian flows and the effect of viscous terms heuristically, neglecting inertia terms, stating that the flow is locally one dimensional and invoking the depth-integrated mass conservation equation, in order to get a nonlinear equation of the free-surface height. The technique has been revisited with the more general asymptotic expansion method: it leads to the same governing equation at zeroth expansion order, but provides a more general theoretical framework for the derivation of reduced models. But only the more complex non-Newtonian case approaches the complexity of both manufacturing processes (concretes, foods) and environmental applications. Concerning slow Bingham fluids, shallow-flow approximations were first studied in 1990 by Liu and Mei [111], based on a rigorous asymptotic expansion. The Liu and Mei approach was revisited in 1999 by Balmforth and Craster [13] and extended [12] to the axisymmetric case, with application to volcanic lava domes. At the beginning of the 21th century, this approach became mature: see [14,6] for some reviews on this subject during this period. Since 2010, many new ideas were developed in several directions: let us review them.

For granular materials, and based on an heuristic derivation, Savage and Hutter [155] developed reduced models. These ideas were revisited in 2014 by Gray and Edwards [90] with a depth-averaged version of the $\mu(I)$-rheology. In 2016, Fernández-Nieto *et al* [71] extended this shallow model as a multi-layer model that allows to compute three-dimensional profiles of the velocity in the directions along and normal to the slope [10].

For fast flows, such as debris and mud flows on mountain slopes, Laigle and Coussot [109,142] derived in 1997 a reduced model, with both inertia and viscoplastic effects. Viscoplastic effects are estimated from the friction at the bottom. In 2009, assuming a compressible material, Bresch *et al* [36,2] derived a reduced viscoplastic model that also includes inertia effects, and the set of equations was solved by an augmented Lagrangian algorithm. This approach was next revisited in the incompressible case in terms of asymptotic analysis [72,73]. In 2010, Ionescu [100] proposed an augmented Lagrangian algorithm for the shallow incompressible viscoplastic model with inertia terms.

While most computations were performed on uniform slopes, practical predictions of natural hazard require to take into account general tridimensional and complex topographies (see e.g. [24]). In 2003, Bouchut *et al* [32, 33] proposed a new approach for topography in shallow flow models, that relaxed most restrictions, such as slowly varying topographies (small curvatures). In 2013, Ionescu [101,102], considering Bingham and Drucker-

Prager models, extended this approach with an elegant formulation based on surface differential operators (surface gradient and divergence) and also included inertia effects. In 2014, Fernández-Nieto [70] studied well-balanced schemes with wet or dry fronts for a viscoplastic model with both topography and inertia effects.

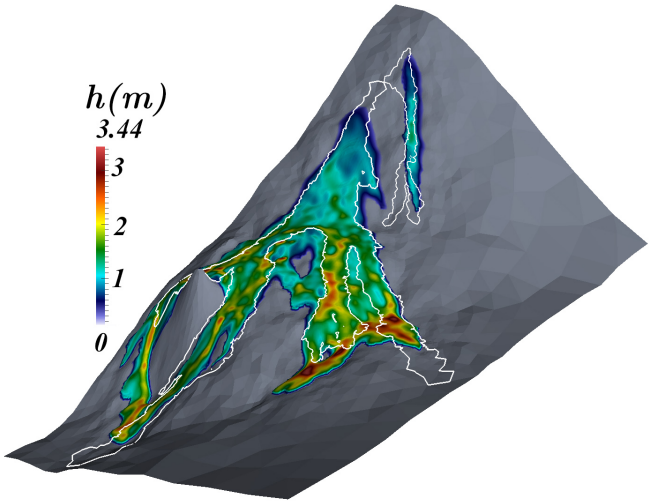

Figure 14 Shallow-flow simulation of the volcanic lava flow predicted flow final deposit represented over the topography, with a color map showing the flow height h (from [25]). The contour of the observed deposit zone provided by the Volcano Observatory of Piton de la Fournaise is represented by a thin white line.

Shallow viscoplastic models with thermal coupling was studied by Balmforth *et al* [15] for lava domes and by Bernabeu *et al* [25] for lava flows on complex tridimensional topographies (See Fig. 14).

Conclusion

Viscoplastic models are widely used in science and engineering to investigate the flow dynamics of fluids with a yield stress. We have presented an extremely large variety of simulation results: many flow geometries, with slip at the wall, with heat transfer, with thixotropy, with elasticity, with multiple phases and for shallow flows. The corresponding rich phenomena observed in these flows are fascinating from a physical viewpoint.

From the simple Bingham model to the most advanced extensions that include temperature dependence, thixotropy or elasticity below the yield stress, the main challenge in numerical simulation remains the treatment of the non-smoothness of the Bingham or Herschel-Bulkley viscoplastic constitutive equation. Hence, the current research direction still pertains to developing new algorithms for the solution of the viscoplastic flow problem with a smaller computational cost while maintaining an accurate description of yield surfaces, at least as accurate as those provided by the augmented Lagrangian algorithm. The revival of augmented Lagrangian methods over the past 10 years and the progressive recognition that they are more accurate than regularization has created a new interest of the viscoplastic community to compute more reliable viscoplastic flow solutions. A simple multi-dimensional Bingham flow problem is a perfect toy problem to test the new family of unregularized approaches that has been recently suggested in the literature: FISTA, Picard fixed point and Newton methods. These different methods all show promises for accelerated convergence, at least for flows in a simple geometry. The next step is now to examine how they perform in more complex geometries and if they can be even further accelerated.

Computational scientists interested in viscoplastic fluid flow simulations call for faster solution algorithms that preserve the accurate resolution of yield surfaces that the classical augmented Lagrangian method guarantees. Combined to new advances in high performance computing on large supercomputers, the milestone of three-dimensional numerical simulation of viscoplastic fluid flows as a standard should be attainable in the next few years.

References

1. S. S. Abdali, E. Mitsoulis, and N. C. Markatos. Entry and exit flows of Bingham fluids. *J. Rheol.*, 36(2):389–407, 1992.
2. C. Acary-Robert, E. D. Fernández-Nieto, G. Narbona-Reina, and P. Vigneaux. A well-balanced finite volume-augmented Lagrangian method for an integrated Herschel-Bulkley model. *J. Sci. Comput.*, 53(3):608–641, 2012.
3. A. Ahmadpour and K. Sadeghy. Start-up flows of Dullaert–Mewis viscoplastic–thixoelastic fluids: a two-dimensional analysis. *J. Non-Newt. Fluid Mech.*, 214:1–17, 2014.
4. A. N. Alexandrou, P. Le Menn, G. C. Georgiou, and V. Entov. Flow instabilities of Herschel–Bulkley fluids. *J. Non-Newt. Fluid Mech.*, 116(1):19–32, 2003.
5. M. Allouche, I. A. Frigaard, and G. Sona. Static wall layers in the displacement of two visco-plastic fluids in a plane channel. *J. Fluid Mech.*, 424:243–277, 2000.
6. C. Ancey. Plasticity and geophysical flows: a review. *J. Non-Newt. Fluid Mech.*, 142:4–35, 2007.
7. C. Ancey, P. Coussot, and P. Evesque. A theoretical framework for granular suspensions in a steady simple shear flow. *J. Rheol.*, 43(6):1673–1699, 1999.
8. A. Aposporidis, E. Haber, M. A. Olshanskii, and A. Veneziani. A mixed formulation of the Bingham fluid flow problem: analysis and numerical solution. *Comput. Meth. Appl. Mech. Engrg.*, 200:2434–2446, 2011.
9. A. Aposporidis, P. S. Vassilevski, and A. Veneziani. Multigrid preconditioning of the non-regularized aug-

mented Bingham fluid problem. *Elect. Trans. Numer. Anal.*, 41:42–61, 2014.
10. E. Audusse and M.-O. Bristeau. Finite-volume solvers for a multilayer Saint-Venant system. *Int. J. Appl. Math. Comput. Sci.*, 17(3):311–320, 2007.
11. R. A. Bagnold. Experiments on a gravity-free dispersion of large solid spheres in a Newtonian fluid under shear. *Proc. R. Soc. Lond. A*, 225:49–63, 1954.
12. N. J. Balmforth, A. S. Burbidge, R. V. Craster, J. Salzig, and A. Shen. Visco-plastic models of isothermal lava domes. *J. Fluid Mech.*, 403:37–65, 2000.
13. N. J. Balmforth and R. V. Craster. A consistent thin-layer theory for Bingham plastics. *J. Non-Newt. Fluid Mech.*, 84(1):65–81, 1999.
14. N. J. Balmforth, R. V. Craster, A. C. Rust, and R. Sassi. Viscoplastic flow over an inclined surface. *J. Non-Newt. Fluid Mech.*, 139:103–127, 2006.
15. N. J. Balmforth, R. V. Craster, and R. Sassi. Dynamics of cooling viscoplastic domes. *J. Fluid Mech.*, 499:149–182, 2004.
16. T. Barker, D. G. Schaeffer, P. Bohorquez, and J. M. N. T. Gray. Well-posed and ill-posed behaviour of the $\mu(I)$-rheology for granular flows. *J. Fluid Mech.*, 779:794–818, 2015.
17. T. Barker, D. G. Schaeffer, P. Bohorquez, J. M. N. T. Gray, and J. Barker. Well-posed continuum modelling of granular flow. In *International congress of theoretical and applied mechanics*, 2016.
18. H. A. Barnes. Thixotropy - a review. *J. Non-Newt. Fluid Mech.*, 70(1):1–33, 1997.
19. A. J. C. Barré de Saint-Venant. Théorie et équations générales du mouvement non permanent des eaux courantes. *C. R. Acad. Sci. Paris*, 73:147–154, 1871.
20. M. Beaulne and E. Mitsoulis. Creeping motion of a sphere in tubes filled with Herschel-Bulkley fluids. *J. Non-Newt. Fluid Mech.*, 72:55–71, 1997.
21. F. Belblidia, H. Tamaddon-Jahromi, M. Webster, and K. Walters. Computations with viscoplastic and viscoelastoplastic fluids. *Rheol. Acta, to appear*, 2011.
22. M. Bercovier and M. Engelman. A finite-element method for incompressible non-Newtonian flows. *J. Comput. Phys.*, 36:313–326, 1980.
23. A. N. Beris, R. C. Armstrong, J. Tsamopoulos, and R. A. Brown. Creeping motion of a sphere through a Bingham plastic. *J. Fluid Mech.*, 158:219–244, 1985.
24. N. Bernabeu, P. Saramito, and C. Smutek. Numerical modeling of shallow non-Newtonian flows: Part II. Viscoplastic fluids and general tridimensional topographies. *Int. J. Numer. Anal. Model.*, 11(1):213–228, 2014.
25. N. Bernabeu, P. Saramito, and C. Smutek. *Modelling lava flow advance using a shallow-depth approximation for three-dimensional cooling of viscoplastic flows*, chapter 27. Geol. Soc., London, 2016.
26. C. R. Beverly and R. I. Tanner. Numerical analysis of three-dimensional Bingham plastic flow. *J. Non-Newt. Fluid Mech.*, 42(1):85–115, 1992.
27. E. C. Bingham. An investigation of the laws of plastic flow. *Bul. Bur. Standards*, 13:309–353, 1916. https://archive.org/details/inv13309353191627827 8unse.
28. E. C. Bingham. *Fluidity and plasticity*. Mc Graw-Hill, New-York, USA, 1922. http://www.archive.org/download/fluidityandplast007721mbp/fluidityandplast007721mbp.pdf.
29. J. Blackery and E. Mitsoulis. Creeping motion of a sphere in tubes filled with a Bingham plastic material. *J. Non-Newt. Fluid Mech.*, 70(1):59–77, 1997.
30. J. Bleyer, M. Maillard, P. de Buhan, and P. Coussot. Efficient numerical computations of yield stress fluid flows using second-order cone programming. *Comput. Meth. Appl. Mech. Engrg.*, 283:599–614, 2015.
31. A. Bose, N. Nirmalkar, and R. P. Chhabra. Forced convection from a heated equilateral triangular cylinder in Bingham plastic fluids. *Numer. Heat Transf. A*, 66(1):107–129, 2014.
32. F. Bouchut, A. Mangeney-Castelnau, B. Perthame, and J.-P. Vilotte. A new model of Saint Venant and Savage-Hutter type for gravity driven shallow water flows. *C. R. Math.*, 336(6):531–536, 2003.
33. F. Bouchut and M. Westdickenberg. Gravity driven shallow water models for arbitrary topography. *Comm. Math. Sci.*, 2(3):359–389, 2004.
34. J. Boujlel, F. Pigeonneau, E. Gouillart, and P. Jop. Rate of chaotic mixing in localized flows. *Phys. Rev. Fluids*, 1(3):031301, 2016.
35. S. P. Boyd and L. Vandenberghe. *Convex optimization*. Cambridge University Press, UK, 2004.
36. D. Bresch, E. D. Fernández-Nieto, I. R. Ionescu, and P. Vigneaux. Augmented Lagrangian method and compressible visco-plastic flows: applications to shallow dense avalanches. In *New directions in mathematical fluid mechanics*, pages 57–89. Springer, 2009.
37. M. G. Cawkwell and M. E. Charles. An improved model for start-up of pipelines containing gelled crude-oil. *J. Pipelines*, 7(1):41–52, 1987.
38. M. G. Cawkwell and M. E. Charles. Characterization of Canadian Arctic thixotropic gelled crude oils utilizing an eight-parameter model. *J. Pipelines*, 7:251–264, 1989.
39. J. Chauchat and M. Médale. A three-dimensional numerical model for incompressible two-phase flow of a granular bed submitted to a laminar shearing flow. *Comput. Meth. Appl. Mech. Engrg.*, 199:439–449, 2010.
40. J. Chauchat and M. Médale. A three-dimensional numerical model for dense granular flows based on the $\mu(I)$ rheology. *J. Comput. Phys.*, 0:to appear, 2013.
41. I. Cheddadi and P. Saramito. A new operator splitting algorithm for elastoviscoplastic flow problems. *J. Non-Newt. Fluid Mech.*, 202:13–21, 2013.
42. I. Cheddadi, P. Saramito, B. Dollet, C. Raufaste, and F. Graner. Understanding and predicting viscous, elastic, plastic flows. *Eur. Phys. J. E*, 34(1):11001, 2011.
43. I. Cheddadi, P. Saramito, and F. Graner. Steady Couette flows of elastoviscoplastic fluids are non-unique. *J. Rheol.*, 56(1):213–239, 2012.
44. I. Cheddadi, P. Saramito, C. Raufaste, P. Marmottant, and F. Graner. Numerical modelling of foam Couette flows. *Eur. Phys. J. E*, 27(2):123–133, 2008.
45. D. C. Cheng. Yield stress: a time-dependent property and how to measure it. *Rheol. Acta*, 25(5):542–554, 1986.
46. S. G. Cherkasov. Combined convection of a viscoplastic liquid in a plane vertical layer. *Fluid Dyn.*, 14(6):901–903, 1979.

47. L. Chupin and T. Dubois. A bi-projection method for Bingham type flows. *submitted*, 2016. https://hal.archives-ouvertes.fr/hal-01166406.
48. P. Coussot. Rheophysics of pastes: a review of microscopic modelling approaches. *Soft Matter*, 3(5):528–540, 2007.
49. Y. Damianou and G. C. Georgiou. Viscoplastic Poiseuille flow in a rectangular duct with wall slip. *J. Non-Newt. Fluid Mech.*, 2014.
50. Y. Damianou, G. Kaoullas, and G. C. Georgiou. Cessation of viscoplastic Poiseuille flow in a square duct with wall slip. *J. Non-Newt. Fluid Mech.*, 233:13–26, 2016.
51. Y. Damianou, M. Philippou, G. Kaoullas, and G. C. Georgiou. Cessation of viscoplastic Poiseuille flow with wall slip. *J. Non-Newt. Fluid Mech.*, 203:24–37, 2014.
52. A. Davaille, B. Gueslin, A. Massmeyer, and E. di Giuseppe. Thermal instabilities in a yield stress fluid: existence and morphology. *J. Non-Newt. Fluid Mech.*, 193:144–153, 2013.
53. G. Daviet and F. Bertails-Descoubes. Nonsmooth simulation of dense granular flows with pressure-dependent yield stress. *J. Non-Newt. Fluid Mech.*, 234:15–35, 2016.
54. J. C. de los Reyes and S. A. González Andrade. Numerical simulation of two-dimensional Bingham fluid flow by semismooth Newton methods. *J. Comput. Appl. Math.*, 235:11–32, 2010.
55. J. C. de los Reyes and S. A. González Andrade. A combined BDF-semismooth Newton approach for time-dependent Bingham flow. *Numer. Meth. Part. Diff. Eqn.*, 28(3):834–860, 2012.
56. J. C. de los Reyes and S. A. González Andrade. Numerical simulation of thermally convective viscoplastic fluids by semismooth second order type methods. *J. Non-Newt. Fluid Mech.*, 193:43–48, 2013.
57. P. R. de Souza Mendes. Thixotropic elasto-viscoplastic model for structured fluids. *Soft Matter*, 7(6):2471–2483, 2011.
58. P. R. de Souza Mendes and R. L. Thompson. A unified approach to model elasto-viscoplastic thixotropic yield-stress materials and apparent yield-stress fluids. *Rheol. Acta*, 52:673–694, 2013.
59. E. J. Dean, R. Glowinski, and G. Guidoboni. On the numerical simulation of Bingham visco-plastic flow: old and new results. *J. Non-Newt. Fluid Mech.*, 142:36–62, 2007.
60. J. J. Derksen and Prashkant. Simulations of complex flow of thixotropic liquids. *J. Non-Newt. Fluid Mech.*, 160(2):65–75, 2009.
61. Y. Dimakopoulos, M. Pavlidis, and J. Tsamopoulos. Steady bubble rise in Herschel–Bulkley fluids and comparison of predictions via the augmented Lagrangian method with those via the Papanastasiou model. *J. Non-Newt. Fluid Mech.*, 200:34–51, 2013.
62. Y. Dimakopoulos and J. Tsamopoulos. Transient displacement of a viscoplastic material by air in straight and suddenly constricted tubes. *J. Non-Newt. Fluid Mech.*, 112(1):43–75, 2003.
63. C. J. Dimitriou, R. H. Ewoldt, and G. H. McKinley. Describing and prescribing the constitutive response of yield stress fluids using large amplitude oscillatory shear stress (LAOStress). *J. Rheol.*, 57(1):27–70, 2013.
64. D. C. Drucker and W. Prager. Soil mechanics and plastic analysis of limit design. *Q. Appl. Math.*, 10:157–175, 1952.
65. K. Dullaert and J. Mewis. Thixotropy: build-up and breakdown curves during flow. *J. Rheol.*, 49(6):1213–1230, 2005.
66. K. Dullaert and J. Mewis. A structural kinetics model for thixotropy. *J. Non-Newt. Fluid Mech.*, 139(1):21–30, 2006.
67. G. Duvaut and J. L. Lions. Transfert de chaleur dans un fluide de Bingham dont la viscosité dépend de la température. *J. Func. Anal.*, 11(1):93–110, 1972.
68. G. Duvaut and J. L. Lions. *Inequalities in mechanics and physics*. Springer, 1976.
69. R. H. Ewoldt, P. Winter, J. Maxey, and G. H. McKinley. Large amplitude oscillatory shear of pseudoplastic and elastoviscoplastic materials. *Rheol. Acta*, 49(2):191–212, 2010.
70. E. D. Fernández-Nieto, J. M Gallardo, and P. Vigneaux. Efficient numerical schemes for viscoplastic avalanches. Part 1: the 1D case. *J. Comput. Phys.*, 264:55–90, 2014.
71. E. D. Fernández-Nieto, J. Garres-Díaz, A. Mangeney, and G. Narbona-Reina. A multilayer shallow model for dry granular flows with the $\mu(I)$ rheology: application to granular collapse on erodible beds. *submitted*, 2016.
72. E. D. Fernández-Nieto, P. Noble, and J.-P. Vila. Shallow water equations for non-Newtonian fluids. *J. Non-Newt. Fluid Mech.*, 165(13):712–732, 2010.
73. E. D. Fernández-Nieto, P. Noble, and J.-P. Vila. Shallow water equations for power law and Bingham fluids. *Sci. China Math.*, 55(2):277–283, 2012.
74. A. Fortin, D. Côté, and P. A. Tanguy. On the imposition of friction boundary conditions for the numerical simulation of Bingham fluid flows. *Comput. Meth. Appl. Mech. Engrg.*, 88(1):97–109, 1991.
75. M. Fortin. *Calcul numérique des écoulements des fluides de Bingham et des fluides newtoniens incompressibles par la méthode des éléments finis*. PhD thesis, Université Paris VI, 1972.
76. M. Fortin and R. Glowinski. *Augmented Lagrangian methods*. Elsevier, 1983.
77. D. Fraggedakis, Y. Dimakopoulos, and J. Tsamopoulos. Yielding the yield-stress analysis: a study focused on the effects of elasticity on the settling of a single spherical particle in simple yield-stress fluids. *Soft Matter*, 2016.
78. I. A. Frigaard and C. Nouar. On the usage of viscosity regularisation methods for visco-plastic fluid flow computation. *J. Non-Newt. Fluid Mech.*, 127(1):1–26, 2005.
79. M. Fuchs, J. F. Grotowski, and J. Reuling. On variational models for quasi-static Bingham fluids. *Math. Meth. Appl. Sci.*, 19(12):991–1015, 1996.
80. M. Fuchs and G. Seregin. Some remarks on non-Newtonian fluids including nonconvex perturbations of the Bingham and Powell–Eyring model for viscoplastic fluids. *Math. Models Meth. Appl. Sci.*, 7(03):405–433, 1997.
81. M. Fuchs and G. Seregin. Regularity results for the quasi–static Bingham variational inequality in dimensions two and three. *Math. Z.*, 227(3):525–541, 1998.
82. M. Fuchs and G. Seregin. *Variational methods for problems from plasticity theory and for generalized Newtonian fluids*. Springer, 2000.

83. P. Fullsack. An arbitrary Lagrangian-Eulerian formulation for creeping flows and its application in tectonic models. *Geophys. J. Int.*, 120(1):1–23, 1995.
84. R. Glowinski. *Lecture on numerical methods for nonlinear variational problems*. Springer, 1980.
85. R. Glowinski and P. Le Tallec. *Augmented Lagrangian and operator splitting methods in nonlinear mechanics*. SIAM, Philadelphia, USA, 1989.
86. R. Glowinski, J. L. Lions, and R. Trémolières. *Numerical analysis of variational inequalities*. Elsevier, 1981.
87. R. Glowinski and A. Wachs. On the numerical simulation of viscoplastic fluid flow. In P. G. Ciarlet and J.-L. Lions, editors, *Handbook of numerical analysis. Volume 16. Numerical methods for non-Newtonian fluids*, chapter 6, pages 483–717. Elsevier, 2011.
88. J. D. Goddard. Dissipative materials as models of thixotropy and plasticity. *J. Non-Newt. Fluid Mech.*, 14:141–160, 1984.
89. R. J. Gordon and W. R. Schowalter. Anisotropic fluid theory: a different approach to the dumbbell theory of dilute polymer solutions. *J. Rheol.*, 16:79–97, 1972.
90. J. M. N. T. Gray and A. N. Edwards. A depth-averaged $\mu(I)$ rheology for shallow granular free-surface flows. *J. Fluid Mech.*, 755:503–534, 2014.
91. P. P. Grinevich and M. A. Olshanskii. An iterative method for the Stokes type problem with variable viscosity. *SIAM J. Sci. Comp.*, 31(5):3959–3978, 2009.
92. I. Henaut and F. Brucy. Description rhéologique des bruts paraffiniques gélifies. In *Congrès du groupe Francais de rhéologie*, 2001.
93. W. H. Herschel and T. Bulkley. Measurement of consistency as applied to rubber-benzene solutions. *Proc. Amer. Soc. Testing Material*, 26(2):621–633, 1926.
94. M. R. Hestenes. Multiplier and gradient methods. *J. Optim. Theory Appl.*, 4(5):303–320, 1969.
95. C. W. Hirt and B. D. Nichols. Volume of fluid (VOF) method for the dynamics of free boundaries. *J. Comput. Phys.*, 39(1):201–225, 1981.
96. S. Hormozi, K. Wielage-Burchard, and I. A. Frigaard. Multi-layer channel flows with yield stress fluids. *J. Non-Newt. Fluid Mech.*, 166(5):262–278, 2011.
97. M. Houska. *Engineering aspects of the rheology of thixotropic liquids*. PhD thesis, Faculty of mechanical engineering, Czech techincal university of Prague, 1981.
98. R. R. Huilgol and G. H. R. Kefayati. Natural convection problem in a Bingham fluid using the operator-splitting method. *J. Non-Newt. Fluid Mech.*, 220:22–32, 2015.
99. H. E. Hupper. The propagation of two-dimensional and axisymmetric viscous gravity currents over a rigid horizontal surface. *J. Fluid Mech.*, 121:43–58, 1982.
100. I. R. Ionescu. Onset and dynamic shallow flow of a viscoplastic fluid on a plane slope. *J. Non-Newt. Fluid Mech.*, 165(19):1328–1341, 2010.
101. I. R. Ionescu. Augmented Lagrangian for shallow viscoplastic flow with topography. *J. Comput. Phys.*, 242:544–560, 2013.
102. I. R. Ionescu and O. Lupaşcu. Modeling shallow avalanche onset over complex basal topography. *Adv. Comput. Math.*, pages 1–22, 2015.
103. I. R. Ionescu, A. Mangeney, F. Bouchut, and O. Roche. Viscoplastic modelling of granular column collapse with pressure and rate dependent viscosity. *J. Non-Newt. Fluid Mech.*, 219:1–18, 2015.
104. P. Jop, Y. Forterre, and O. Pouliquen. A constitutive law for dense granular flows. *Nature*, 441:727–730, 2006.
105. I. Karimfazli, I. A. Frigaard, and A. Wachs. A novel heat transfer switch using the yield stress. *J. Fluid Mech.*, 783:526–566, 2015.
106. I. Karimfazli, I. A. Frigaard, and A. Wachs. Thermal plumes in viscoplastic fluids: flow onset and development. *J. Fluid Mech.*, 787:474–507, 2016.
107. A. J. C. Ladd and R. Verberg. Lattice-Boltzmann simulations of particle-fluid suspensions. *J. Stat. Phys.*, 104(5):1191–1251, 2001.
108. P.-Y. Lagrée, L. Staron, and S. Popinet. The granular column collapse as a continuum: validity of a two-dimensional Navier–Stokes model with a $\mu(I)$-rheology. *J. Fluid Mech.*, 686:378–408, 2011.
109. D. Laigle and P. Coussot. Numerical modeling of mudflows. *J. Hydr. Engrg.*, 123(7):617–623, 1997.
110. J.-C. Latché and D. Vola. Analysis of the Brezzi-Pitkäranta stabilized Galerkin scheme for creeping flows of Bingham fluids. *SIAM J. Numer. Anal.*, 42(3):1208–1225, 2005.
111. K. F. Liu and C. C. Mei. Approximation equations for the slow spreading of a thin Bingham plastic fluid. *Phys. Fluids A*, 2(1):30–36, 1990.
112. Y. Liu, N. J. Balmforth, S. Hormozi, and D. R. Hewitt. Two–dimensional viscoplastic dambreaks. *J. Non-Newt. Fluid Mech.*, in press, 2016.
113. A. Maleki, S. Hormozi, A. Roustaei, and I. A. Frigaard. Macro-size drop encapsulation. *J. Fluid Mech.*, 769:482–521, 2015.
114. GDR Midi. On dense granular flows. *Eur. Phys. J. E*, 14(4):341–365, 2004.
115. E. Mitsoulis, S. S. Abdali, and N. C. Markatos. Flow simulation of Herschel-Bulkley fluids through extrusion dies. *Can. J. Chem. Engrg.*, 71:147–160, 1993.
116. E. Mitsoulis and R. R. Huilgol. Entry flows of Bingham plastics in expansions. *J. Non-Newt. Fluid Mech.*, 122:45–54, 2004.
117. E. Mitsoulis and J. Tsamopoulos. Numerical simulation of complex yield stress fluid flows. *Rheol. Acta*, submitted, 2016.
118. R. Mittal and G. Iaccarino. Immersed boundary methods. *Annu. Rev. Fluid Mech.*, 37:239–261, 2005.
119. F Moore. The rheology of ceramic slips and bodies. *Trans. British Ceramics Soc.*, 58:470–494, 1959.
120. P. P. Mosolov and V. P. Miasnikov. Variational methods in the theory of the fluidity of a viscous-plastic medium. *J. Appl. Math. Mech.*, 29(3):545–577, 1965.
121. P. P. Mosolov and V. P. Miasnikov. On stagnant flow regions of a viscous-plastic medium in pipes. *J. Appl. Math. Mech.*, 30(4):841–853, 1966.
122. P. P. Mosolov and V. P. Miasnikov. On qualitative singularities of the flow of a viscoplastic medium in pipes. *J. Appl. Math. Mech.*, 31(3):609–613, 1967.
123. M. A. Moyers-Gonzalez and I. A. Frigaard. Numerical solution of duct flows of multiple visco-plastic fluids. *J. Non-Newt. Fluid Mech.*, 127:227–241, 2004.
124. A. Mujumdar, A. N. Beris, and A. B. Metzner. Transient phenomena in thixotropic systems. *J. Non-Newt. Fluid Mech.*, 102:157–178, 2002.
125. E. Muravleva and M. A. Olshanskii. Two finite-difference schemes for calculation of Bingham fluid flows

in a cavity. *Russ. J. Numer. Anal. Math. Modelling*, 23(6):615–634, 2008.
126. L. Muravleva. Uzawa-like methods for numerical modeling of unsteady viscoplastic Bingham medium flows. *Appl. Numer. Math.*, 93:140–149, 2015.
127. L. Muravleva, E. Muravleva, G. C. Georgiou, and E. Mitsoulis. Numerical simulations of cessation flows of a Bingham plastic with the augmented Lagrangian method. *J. Non-Newt. Fluid Mech.*, 165:544–550, 2010.
128. C. O. R. Negrão, A. T. Franco, and L. L. V. Rocha. A weakly compressible flow model for the restart of thixotropic drilling fluids. *J. Non-Newt. Fluid Mech.*, 166(23):1369–1381, 2011.
129. K. D. Nikitin, M. A. Olshanskii, K. M. Terekhov, and Y. V. Vassilevski. Numerical method for the simulation of free surface flows of viscoplastic fluid in 3D. *J. Comput. Math.*, 29:605–622, 2011.
130. N. Nirmalkar, A. Bose, and R. P. Chhabra. Free convection from a heated circular cylinder in Bingham plastic fluids. *Int. J. Thermal Sci.*, 83:33–44, 2014.
131. N. Nirmalkar, R. P. Chhabra, and R. J. Poole. Laminar forced convection heat transfer from a heated square cylinder in a Bingham plastic fluid. *Int. J. Heat Mass Transf.*, 56(1):625–639, 2013.
132. J. G. Oldroyd. A rational formulation of the equations of plastic flow for a Bingham fluid. *Proc. Cambridge Philos. Soc.*, 43:100–105, 1947.
133. J. G. Oldroyd. On the formulation of rheological equations of states. *Proc. R. Soc. Lond. A*, 200:523–541, 1950.
134. M. A. Olshanskii. Analysis of semi-staggered finite-difference method with application to Bingham flows. *Comput. Meth. Appl. Mech. Engrg.*, 198:975–985, 2009.
135. G. Ovarlez, Q. Barral, and P. Coussot. Three-dimensional jamming and flows of soft glassy materials. *Nature Mat.*, 9:115–119, 2010.
136. T. C. Papanastasiou. Flow of materials with yield. *J. Rheol.*, 31:385–404, 1987.
137. Y. S. Park and P. L.-F. Liu. Oscillatory pipe flows of a yield-stress fluid. *J. Fluid Mech.*, 658:211–228, 2010.
138. M. J. D. Powell. *A method for nonlinear constraints in minimization problems*, pages 283–298. Academic Press, London, 1969.
139. Prashant and J. J. Derksen. Direct simulations of spherical particle motion in Bingham liquids. *Comput. Chem. Engrg.*, 35(7):1200–1214, 2011.
140. A. Putz and I. A. Frigaard. Creeping flow around particle in a Bingham fluid. *J. Non-Newt. Fluid Mech.*, 165(5–6):263–280, 2010.
141. A. Putz, I. A. Frigaard, and D. M. Martinez. On the lubrication paradox and the use of regularisation methods for lubrication flows. *J. Non-Newt. Fluid Mech.*, 163:62–77, 2009.
142. D. Rickenmann, D. Laigle, B. W. McArdell, and J. Hübl. Comparison of 2D debris-flow simulation models with field events. *Comput. Geo.*, 10(2):241–264, 2006.
143. R. T. Rockafellar. Augmented Lagrangians and applications of the proximal point algorithm in convex programming. *Math. Oper. Res.*, 1(2):97–116, 1976.
144. N. Roquet and P. Saramito. An adaptive finite element method for Bingham fluid flows around a cylinder. *Comput. Meth. Appl. Mech. Engrg.*, 192(31-32):3317–3341, 2003.
145. N. Roquet and P. Saramito. An adaptive finite element method for viscoplastic flows in a square pipe with stick-slip at the wall. *J. Non-Newt. Fluid Mech.*, 155:101–115, 2008.
146. A. Roustaei and I. A. Frigaard. The occurrence of fouling layers in the flow of a yield stress fluid along a wavy-walled channel. *J. Non-Newt. Fluid Mech.*, 198:109–124, 2013.
147. A. Roustaei, A. Gosselin, and I. A. Frigaard. Residual drilling mud during conditioning of uneven boreholes in primary cementing. Part 1: rheology and geometry effects in non-inertial flows. *J. Non-Newt. Fluid Mech.*, 220:87–98, 2015.
148. P. Saramito. Numerical simulation of viscoelastic fluid flows using incompressible finite element method and a θ-method. *Math. Model. Numer. Anal.*, 28(1):1–35, 1994.
149. P. Saramito. A new constitutive equation for elastoviscoplastic fluid flows. *J. Non-Newt. Fluid Mech.*, 145(1):1–14, 2007.
150. P. Saramito. A new elastoviscoplastic model based on the Herschel-Bulkley viscoplasticity. *J. Non-Newt. Fluid Mech.*, 158(1–3):154–161, 2009.
151. P. Saramito. *Complex fluids: modelling and algorithms*. Springer, 2016.
152. P. Saramito. A damped Newton algorithm for computing viscoplastic fluid flows. *J. Non-Newt. Fluid Mech.*, in press, 2016. https://hal.archives-ouvertes.fr/hal-01228347/document.
153. P. Saramito and N. Roquet. An adaptive finite element method for viscoplastic fluid flows in pipes. *Comput. Meth. Appl. Mech. Engrg.*, 190(40-41):5391–5412, 2001.
154. S. B. Savage. The mechanics of rapid granular flows. *Adv. Appl. Mech.*, 24:289–366, 1984.
155. S. B. Savage and K. Hutter. The motion of a finite mass of granular material down a rough incline. *J. Fluid Mech.*, 199:177–215, 1989.
156. R. S. Schechter and E. H. Wissler. Heat transfer to Bingham plastics in laminar flow through circular tubes with internal heat generation. *Nuclear Sci. Engrg.*, 6(5):371–375, 1959.
157. T. Schwedoff. La rigidité des liquides. In *Congrès Int. Physique, Paris*, volume 1, pages 478–486, 1900.
158. J. Sestak, M. E. Charles, M. G. Cawkwell, and M. Houska. Start-up of gelled crude oil pipelines. *J. Pipelines*, 6(1):15–24, 1987.
159. J. P. Singh and M. M. Denn. Interacting two-dimensional bubbles and droplets in a yield-stress fluid. *Phys. Fluids*, 20(4):040901, 2008.
160. D. N. Smyrnaios and J. Tsamopoulos. Squeeze flow of Bingham plastics. *J. Non-Newt. Fluid Mech.*, 100(1):165–189, 2001.
161. M. Sussman, P. Smereka, and S. Osher. A level set approach for computing solutions to incompressible two-phase flow. *J. Comput. Phys.*, 114:146–159, 1994.
162. A. Syrakos, G. C. Georgiou, and A. N. Alexandrou. Performance of the finite volume method in solving regularised Bingham flows: inertia effects in the lid-driven cavity flow. *J. Non-Newt. Fluid Mech.*, 208:88–107, 2014.

163. P. Szabo and O. Hassager. Flow of viscoplastic fluids in eccentric annular geometries. *J. Non-Newt. Fluid Mech.*, 45(2):149–169, 1992.
164. P. Szabo and O. Hassager. Displacement of one Newtonian fluid by another: density effects in axial annular flow. *Int. J. Multiphase Flow*, 23(1):113–129, 1997.
165. R. I. Tanner and K. Walters. *Rheology: an historical perspective*. Elsevier, 1998.
166. D. L. Tokpavi, A. Magnin, and P. Jay. Very slow flow of Bingham viscoplastic fluid around a circular cylinder. *J. Non-Newt. Fluid Mech.*, 154(1):65–76, 2008.
167. T. Treskatis, M. A. Moyers-Gonzalez, and C. J. Price. A trust-region SQP method for the numerical approximation of viscoplastic fluid flow. *submitted*, 2015. http://arxiv.org/pdf/1504.08057.pdf.
168. T. Treskatis, M. A. Moyers-Gonzalez, and C. J. Price. An accelerated dual proximal gradient method for applications in viscoplasticity. *J. Non-Newt. Fluid Mech.*, in press, 2016.
169. M. K. Tripathi, K. C. Sahu, G. Karapetsas, and O. K. Matar. Bubble rise dynamics in a viscoplastic material. *J. Non-Newt. Fluid Mech.*, 222:217–226, 2015.
170. J. Tsamopoulos, Y. Dimakopoulos, N. Chatzidai, G. Karapetsas, and M. Pavlidis. Steady bubble rise and deformation in Newtonian and viscoplastic fluids and conditions for bubble entrapment. *J. Fluid Mech.*, 601:123–164, 2008.
171. O. Turan, N. Chakraborty, and R. J. Poole. Laminar natural convection of Bingham fluids in a square enclosure with differentially heated side walls. *J. Non-Newt. Fluid Mech.*, 165(15):901–913, 2010.
172. O. Turan, R. J. Poole, and N. Chakraborty. Aspect ratio effects in laminar natural convection of Bingham fluids in rectangular enclosures with differentially heated side walls. *J. Non-Newt. Fluid Mech.*, 166(3):208–230, 2011.
173. S. O. Unverdi and G. Tryggvason. A front-tracking method for viscous, incompressible, multi-fluid flows. *J. Comput. Phys.*, 100(1):25–37, 1992.
174. A. Vikhansky. Thermal convection of a viscoplastic liquid with high Rayleigh and Bingham numbers. *Phys. Fluids*, 21(10):103103, 2009.
175. A. Vikhansky. On the onset of natural convection of Bingham liquid in rectangular enclosures. *J. Non-Newt. Fluid Mech.*, 165(23):1713–1716, 2010.
176. A. Vikhansky. On the stopping of thermal convection in viscoplastic liquid. *Rheol. Acta*, 50(4):423–428, 2011.
177. G. Vinay, A. Wachs, and J.-F. Agassant. Numerical simulation of non-isothermal viscoplastic waxy crude oil flows. *J. Non-Newt. Fluid Mech.*, 128(2):144–162, 2005.
178. D. Vola, F. Babik, and J.-C. Latché. On a numerical strategy to compute gravity currents of non-Newtonian fluids. *J. Comput. Phys.*, 201(2):397–420, 2004.
179. D. Vola, L. Boscardin, and J.-C. Latché. Laminar unsteady flows of Bingham fluids: a numerical strategy and some benchmark results. *J. Comput. Phys.*, 187:441–456, 2003.
180. A. Wachs. Numerical simulation of steady Bingham flow through an eccentric annular cross-section by distributed Lagrange multiplier/fictitious domain and augmented Lagrangian methods. *J. Non-Newt. Fluid Mech.*, 142:183–198, 2007.
181. A. Wachs and I. A. Frigaard. Particle settling in yield stress fluids: limiting time, distance and applications. *J. Non-Newt. Fluid Mech.*, in press, 2016.
182. A. Wachs, G. Vinay, and I. A. Frigaard. A 1.5D numerical model for the start up of weakly compressible flow of a viscoplastic and thixotropic fluid in pipelines. *J. Non-Newt. Fluid Mech.*, 159(1):81–94, 2009.
183. S. D. R. Wilson and A. J. Taylor. The channel entry problem for a yield stress fluid. *J. Non-Newt. Fluid Mech.*, 65:165–176, 1996.
184. W. J. Yang and H. C. Yeh. Free convective flow of Bingham plastic between two vertical plates. *J. Heat Transf.*, 87(2):319–320, 1965.
185. Z. Yu and A. Wachs. A fictitious domain method for dynamic simulation of particle sedimentation in Bingham fluids. *J. Non-Newt. Fluid Mech.*, 145:78–91, 2007.
186. J. Zhang. An augmented Lagrangian approach to Bingham fluid flows in a lid-driven square cavity with piecewise linear equal-order finite elements. *Comput. Meth. Appl. Mech. Engrg.*, 199:3051–3057, 2010.
187. J. Zhang, D. Vola, and I. A. Frigaard. Yield stress effects on Rayleigh-Bénard convection. *J. Fluid Mech.*, 566:389–420, 2006.
188. Y. Zhang. Error estimates for the numerical approximation of time-dependent flow of Bingham fluid in cylindrical pipes by the regularization method. *Numer. Math.*, 96:153–184, 2003.
189. T. Zisis and E. Mitsoulis. Viscoplastic flow around a cylinder kept between parallel plates. *J. Non-Newt. Fluid Mech.*, 105:1–20, 2002.